Natural Resources Canada | Ressources naturelles Canada

GEOLOGICAL SURVEY OF CANADA
OPEN FILE 9182

Source-rock potential of samples from Bylot Island, Nunavut

J.B.W. Wielens, J.W. Haggart, A.M. Kalejaiye, M. Obermajer, O. Khriashchevska, K.E. Dewing, and C. Jiang

2024

Canada

GEOLOGICAL SURVEY OF CANADA
OPEN FILE 9182

Source-rock potential of samples from Bylot Island, Nunavut

J.B.W. Wielens*, J.W. Haggart, A.M. Kalejaiye, M. Obermajer,
O. Khriashchevska, K.E. Dewing, and C. Jiang

*Deceased (1948–2010)

2024

Recommended citation:
Wielens, J.B.W., Haggart, J.W., Kalejaiye, A.M., Obermajer, M., Khriashchevska, O., Dewing, K.E., and Jiang, C., 2024. Source-rock potential of samples from Bylot Island, Nunavut; Geological Survey of Canada, Open File 9182, 39 p. https://doi.org/10.4095/pwj9f8bdjc

Publications in this series have not been edited; they are released as submitted by the authors.

ISSN 2816-7155
ISBN 978-0-660-72595-6
Catalogue No. M183-2/9182E-PDF
https://doi.org/10.4095/pwj9f8bdjc

EXECUTIVE SUMMARY

Cretaceous and Cenozoic samples, in addition to samples of other ages collected on Bylot Island, Nunavut were examined for source rock potential to evaluate different indications of the presence of a petroleum system in the area. Rock-Eval and vitrinite reflectance analyses were conducted for these samples collected from outcrops on the island during field trips by GSC and university researchers. The results revealed the presence of Type III source rocks with TOC ranging between 1-56%, however most of the samples are immature with respect to hydrocarbon generation (below 0.5% VRo and average Tmax of 425ºC).

The results of these analyses are valuable for hydrocarbon resource assessment of the eastern Canadian Arctic margin, needed to initiate discussions for Marine Protected Areas for the Canadian government to meet its carbon net zero objectives by 2050.

Table of Contents

INTRODUCTION

Cretaceous oil seeps in western Greenland (Bojesen-Koefoed et al., 1999) and a Late Cretaceous oil seep at Scott Inlet off NE Baffin Island (Moir et al. 2012) imply the presence of mature source rocks within the Baffin Bay and the Davis Strait. In addition, several wells drilled in the Labrador Sea found hydrocarbons with the Cretaceous age Bjarni Formation as the major source rock (Carey et al. 2020). Additional work with RADARSAT has shown oil slicks in the Labrador Sea and Baffin Bay (Oakey et al. 2012; Decker et al., 2013).

Bylot Island was chosen for Rock-Eval analysis of Cretaceous and Cenozoic formations because it is one of the few places where rocks of this age outcrop in the region. The aim of these analyses is to assess the presence and potential of the source element of petroleum systems. If this petroleum system element is present on the island, then the likelihood of a source rock being present in the offshore is much higher. Understanding source rock parameters and distribution will increase the certainty of source rock presence and quality which appeared to be the main risk in Lancaster Sound and Davis Strait.

PREVIOUS WORK

In the 1970s, Jackson and Davidson (1975a, b) and Jackson et al. (1975) mapped the Mesozoic-Cenozoic strata preserved on SW Bylot Island. They called the strata Eclipse Group and assigned them to Early Cretaceous – Eocene age, based on preliminary biostratigraphic analysis. Other researchers subsequently studied Bylot Island to better understand the stratigraphic setting, regional extent and resource potential of the rocks. Miall et al., (1980) mainly focused on the south coast and Twosnout Creek areas of the island; he produced a schematic geological map and expanded stratigraphic framework of the Cretaceous–Cenozoic sedimentary succession. Elliot Burden and students from Memorial University of Newfoundland carried out fieldwork on Bylot Island in the 1980s (e.g., Waterfield, 1989; Burden and Langille, 1990). The GSC carried out fieldwork in 2009. This work has been recently summarized in Currie et al. (2020), who correlated stratigraphy between Bylot Island and the near offshore and Haggart et al. (2022) who summarize the geology of all Cretaceous-Paleocene strata along western Baffin Bay.

Jackson and Sangster (1987) examined the Proterozoic rocks on Bylot Island and described them to be petroliferous having minute bitumen blebs in trace amounts throughout much of the Society Cliffs Formation, Athole Point Formation and locally in the Victor Bay Formation. One Athole Point sample indicated traces of oil when examined with ultraviolet light. The stratigraphy of the Mesoproterozoic basin has been summarized by Turner (2009).

GEOLOGICAL SETTING

Bylot Island (Fig. 1) is located northeast of Baffin Island. The centre of the island is characterized by Archean rocks whereas outcrops of Mesozoic to Cenozoic age are present on the North and South of the island in a down-faulted grabens. These outcrops preserve stratigraphic evidence of the depositional and tectonic evolution of western Baffin Bay and are the analogues for strata underlying part of the continental shelf and slope off the coast of Bylot Island (Haggart et al., 2022). Miall et al (1980) divided

Cretaceous strata into the Early Cretaceous sandstone dominated Hassel Formation, and Upper Cretaceous mudstone dominated Kanguk Formation that has a locally developed upper sandy member. Portions of the Hassel Formation were deposited in a fluvial setting, whereas other parts of the Hassel Formation and the Kanguk Formation were deposited in marine settings. Rocks of the overlying Paleocene Eureka Sound Formation (Miall et al, 1980) consist of a locally developed lower sandstone member, a lower mudstone member, upper sandstone member and upper mudstone member. These were deposited in fluvial, deltaic and very shallow marine settings.

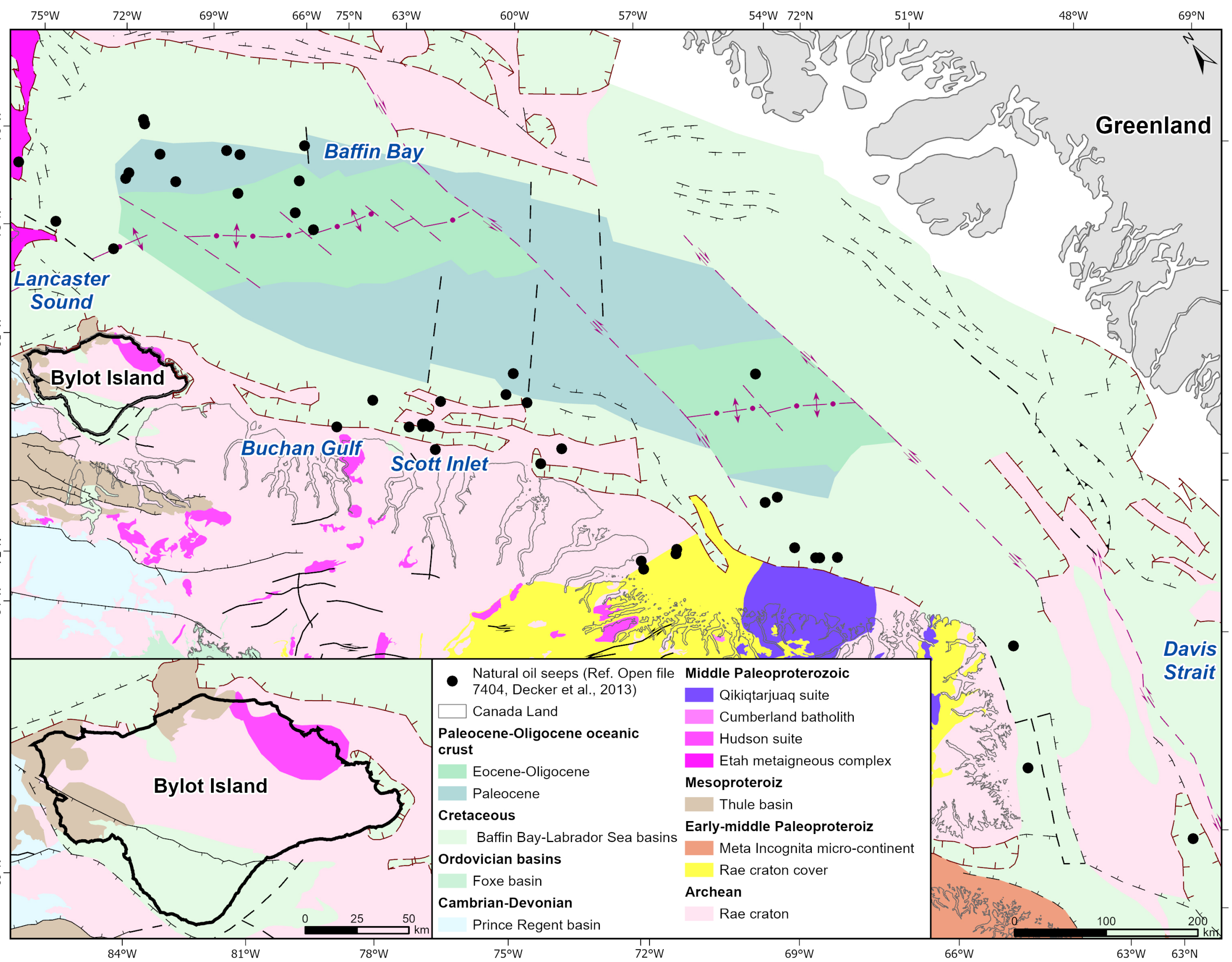

Figure 1. Regional geological map of the study area showing natural oil seeps locations.

METHODOLOGY

Pyrolysis experiments were conducted using a Rock-Eval VI equipped with a total organic carbon module. A Rock-Eval run starts by heating a pulverized rock sample at 300ºC for 3 min in helium atmosphere, during which free and adsorbed hydrocarbons are volatilized. Then the oven temperature increases to 600ºC at a rate of 25ºC/min and decomposition of kerogen occurs. The final stage involves oxidation and combustion of the residual organic matter at 600ºC. The amount of hydrocarbons volatilized at 300ºC and evolved from kerogen at 300ºC to 600ºC is measured by a flame ionization detector, and recorded as the S1 and S2 peaks, respectively. The temperature measured at the maximum of the S2 peak is referred to as Tmax. The quantity of organic CO2 generated from 300ºC to 390ºC, determined by a thermal conductivity detector, comprises the S3 peak. The percentage of carbon in CO_2 formed during oxidation at 600ºC and in the hydrocarbon peaks S1 and S2 is used to define the total organic carbon content (TOC). The quality of organic matter is based upon the calculation of Hydrogen (HI) and Oxygen (OI) indices (HI=S2/TOCx100, OI=S3/TOCx100) which are related to the atomic H/C and O/C ratios. The OI versus HI cross plots ("pseudo van Krevelen diagrams") can be used as an organic matter type indicator at low and moderate maturities. The Tmax is an indicator of relative thermal maturity and can be converted to a vitrinite equivalent reflectance using Jarvie's equation (Jarvie, 2018).

ROCK EVAL RESULTS

There are 236 Rock-Eval analyses from Bylot Island in the GSC sample management database. Of these, 69 are from Proterozoic strata of the Borden Basin collected by university researchers, two are from lower Paleozoic strata, 67 were collected during the 1970s (Miall et al., 1980), 24 are from samples originating from Elliot Burden and processed by Hans Wielens, and 74 were collected by Hans Wielens and colleagues in 2009. Figures 2a and 2b show the locations of samples, and Table A-1 in Appendix A gives the latitude and longitude together with the analytical results. Note that samples preface with HFB09 were renamed to WIA09 for the Rock-Eval analysis.

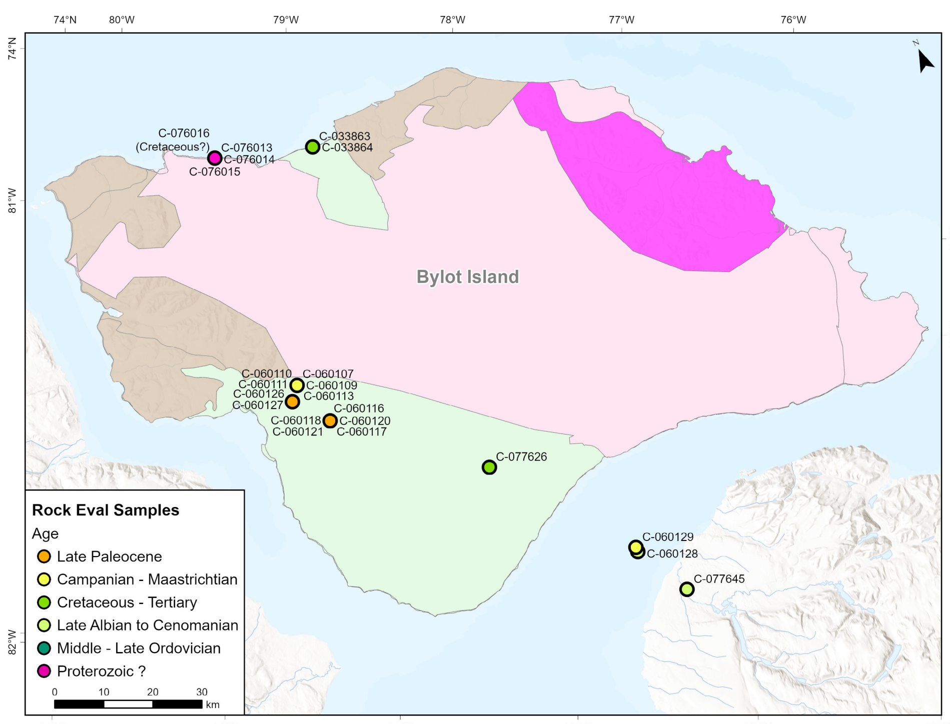

Figure 2a. Known age sample locations.

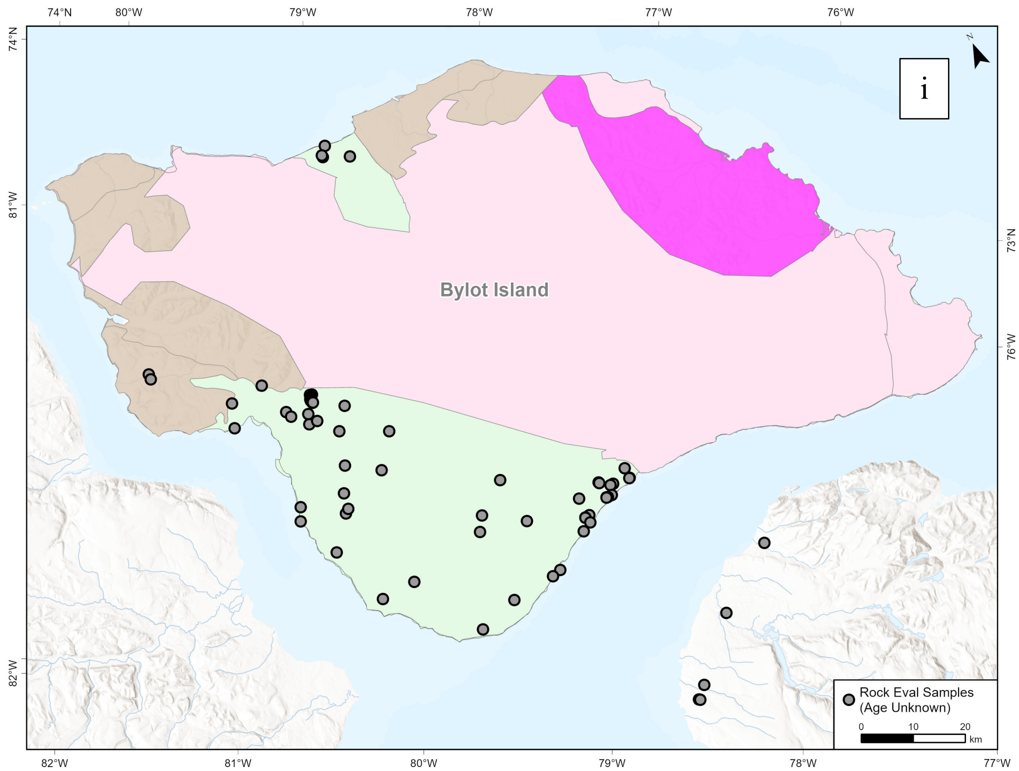

Figure 2b. Unknown age sample locations.

Samples from Proterozoic strata were reported in Fustic et al. (2017). The TOC averages 1.9 wt.%, with very low S2 (Fig. 3; Table A-1 in Appendix A) and high residual carbon (RC%). Tmax averages 564 °C for samples in the range 450-600 °C that also have S2>0.2 mg HC/g rock (Fig. 3). Note that the pyrolysis experiments end at 610 °C which means that Tmax of greater than 600 °C exceed the instrument calibration.

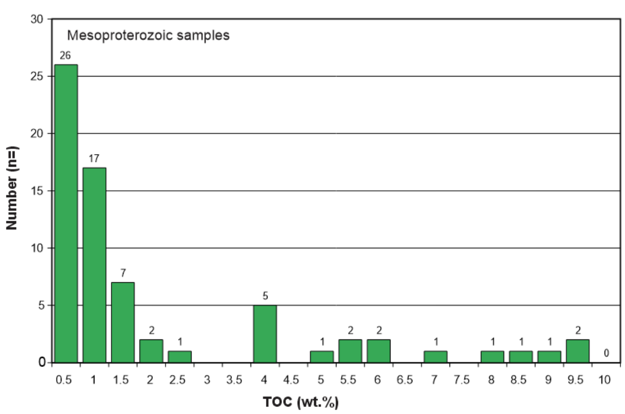

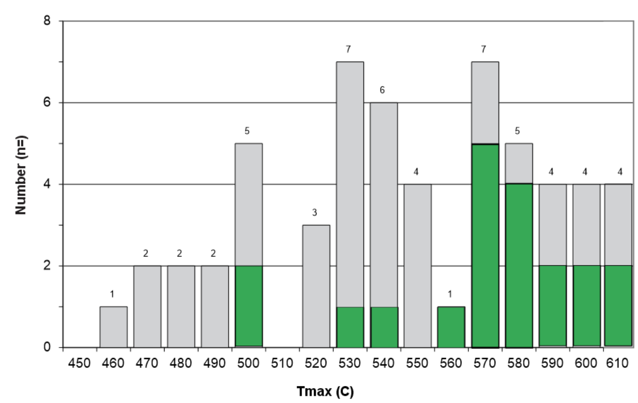

Figure 3. Proterozoic samples from Bylot Island (Fustic et al. 2017). Left: Histogram of TOC (wt%); Right: Histogram of Tmax (°C) between 450 and 610 °C. Bin 450 indicates number of samples with Tmax less than 450°C. Samples with S2 greater than 0.2 mg HC/g rock shown in green.

There are 156 Cretaceous and Cenozoic samples between 0-10 wt.% TOC; these have an average TOC of 1.58 wt.%. 11 coaly samples with TOC in the range 11-53 wt.% have an average TOC of 32.9 wt.% (Fig. 4). Average S2 is 2.4 mg HC/g rock. HI vs OI (pseudo van Krevelen diagram; Fig. 5) indicates a dominant Type III kerogen. The highest HI value of 292 is from sample C-77626 collected from undivided Hassel-Kanguk formations has a TOC of 0.25 wt.%. Average Tmax for samples with S2 greater than 0.2 mg HC/g rock is 425 °C (Fig. 6.)

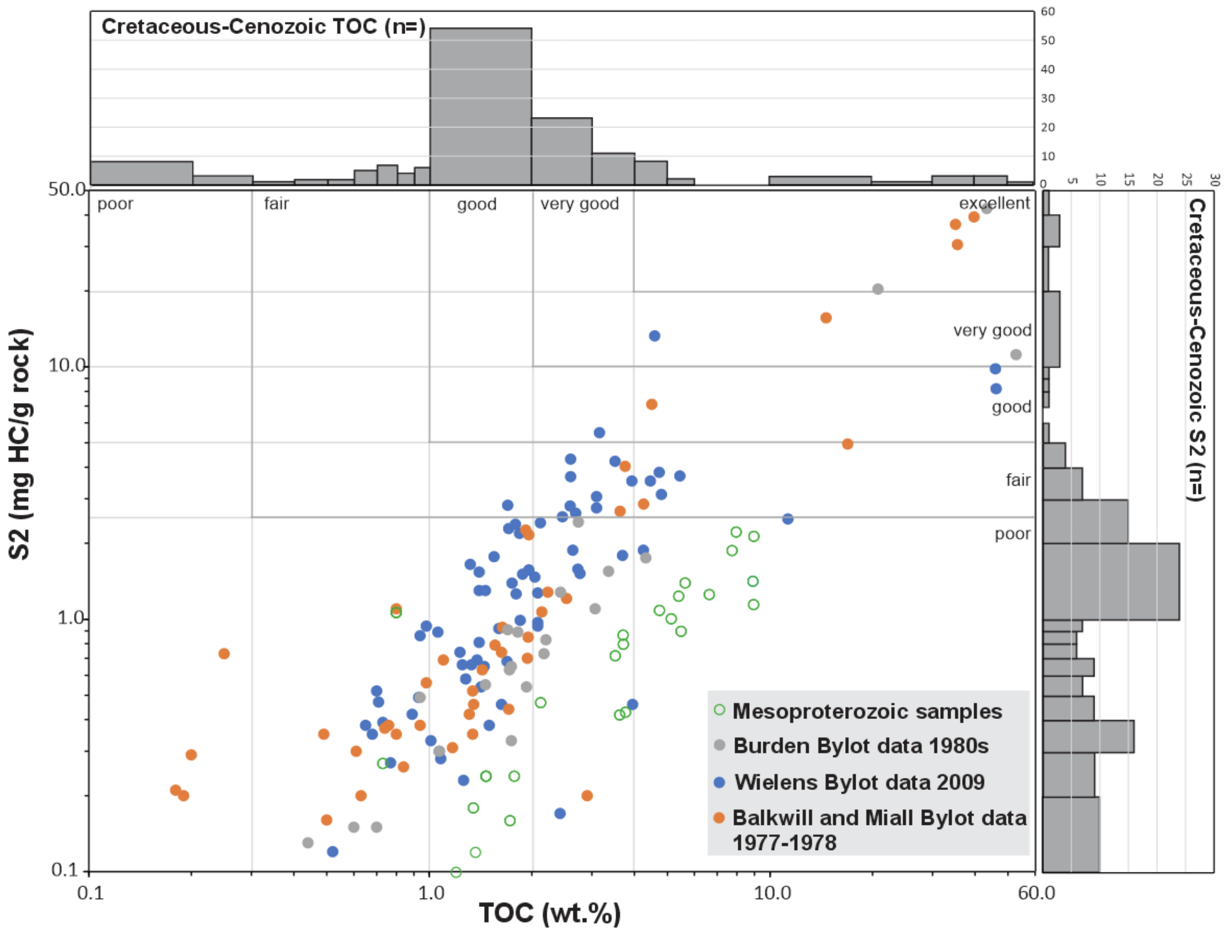

Figure 4. TOC (wt.%) vs. S2 (mg HC/g rock) of Cretaceous-Cenozoic samples (solid fill) and Proterozoic sample (empty circles). Histograms for TOC and S2 of Cretaceous-Cenozoic samples are shown above and to the right of the cross plot. Balkwill and Miall Bylot data 1977-1978 located in Miall et al (1980)

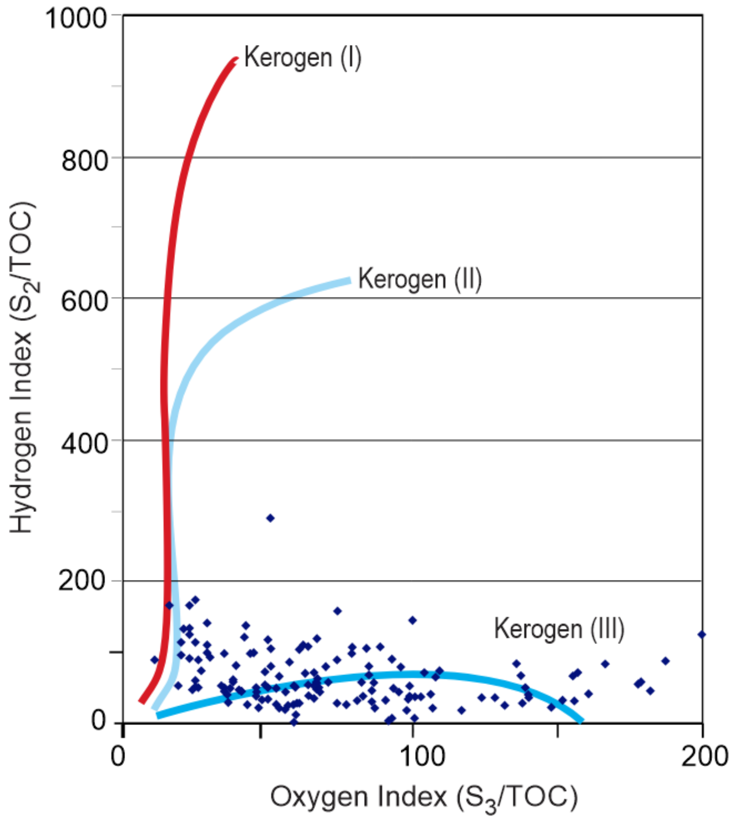

Figure 5. Hydrogen Index vs Oxygen Index for Cretaceous-Cenozoic samples fall on the Type III kerogen curve.

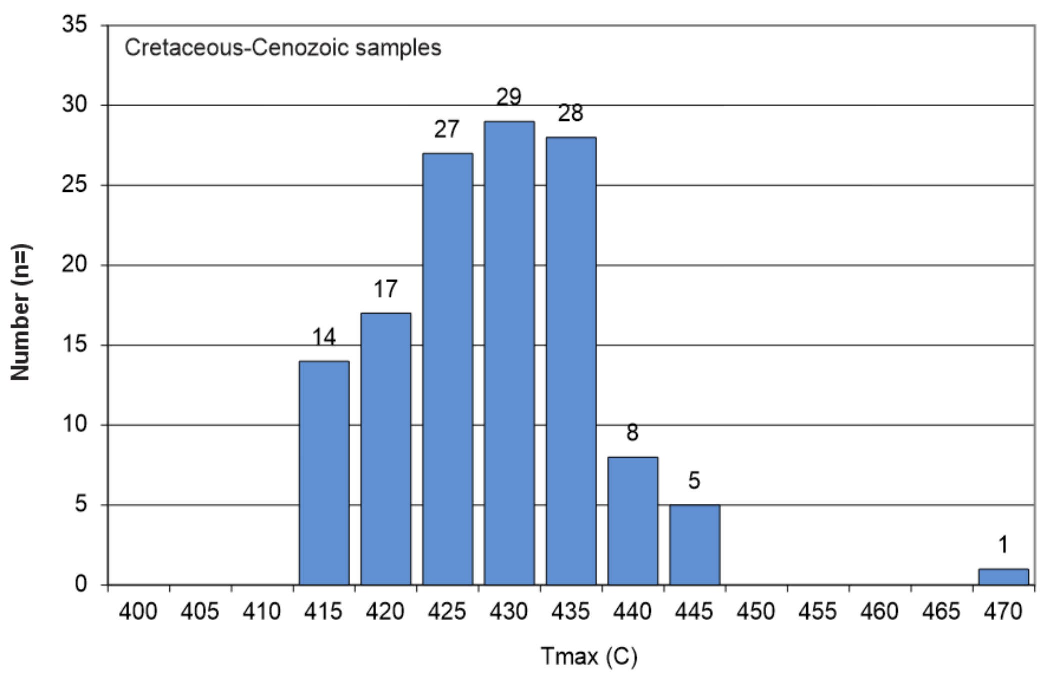

Figure 6. Histogram of Tmax for Cretaceous-Cenozoic samples with S2 greater than 0.2 mg HC/g rock. Average Tmax is 425°C. Bin 415 includes all samples with Tmax 410-415°C.

HYDROCARBON EXTRACT

The method of this analysis is non-standard, and the steps taken to process this sample is described below.

About 10 g of a hand-pulverized coaly sample (See Table 1) collected from the Hassel Formation exposed along the Salmon River near Pond Inlet on northern Baffin Island (collector/reference; GSC C-77645; X11354) (TOC of 37.42%) were Soxhlet-extracted for 24 hours using approximately 350 ml of an azeotropic mixture of 87% chloroform and 13% methanol. About 379 mg of total organic extract were obtained after the solvent was removed in a rotary evaporator (temperature set at 35°-40°C). The extract was dissolved in chloroform, treated with colloidal copper to remove elemental sulphur, filtered through glass fibre filter paper to remove the copper sulphide and excess copper, rotary-evaporated and dried. The total extract yield, normalized to the organic matter content (TOC) and expressed as milligrams of total extract per gram of organic carbon, is 100.96 mg/g TOC. The extract was then dissolved in a minimal amount of chloroform, treated with pentane to precipitate asphaltenes and then vacuum filtered to remove the precipitate. The asphaltenes were dissolved in chloroform, collected to a separate tared flask, rotary-evaporated and weighted to constant weight.

The resulting extract was fractionated using open-column liquid chromatography. A mixture of 28-200 mesh Silica Gel (MCB) and 80-200 mesh alumina (ALCOA) (1/3:2/3 by weight, respectively) was used as adsorbents for the column. The adsorbents, activated by heating at 120-150 °C for 12 hours, were weighed as 1 g of adsorbents/10 mg of extract and then slowly settled in pentane. A de-asphalted extract, dissolved in a minimal amount of previously measured pentane, was then added to the column. Saturates were recovered by eluting with pentane (3.5 ml/g adsorbents), aromatics with a 50:50 mixture of pentane and dichloromethane (4 ml/g adsorbents), NSO (Nitrogen Sulphur Oxygen) compounds with methanol (4 ml/g adsorbents) and the remaining asphaltene fraction was retrieved using chloroform. The hydrocarbon fractions (saturate and aromatics) were treated again with colloidal copper as sulphur was still present after fractionation. The solvents were rotary-evaporated, separate fractions transferred to tared 1dram vials, dried in a slow stream of nitrogen and weighted to constant weight.

The fractionation resulted in obtaining 3.15 mg of hydrocarbons (saturates 1 mg, aromatics 2.15 mg), 23.78 mg of NSO's and 261 mg of asphaltenes. Overall, the recovery rate was just below 80%, which is low for this type of analytical process. The composition of the extract, normalized to the extract weight after fractionation is as follows: saturates 1.27%, aromatics 2.72%, NSO's 8% and asphaltenes 88%. The hydrocarbon yield is 3.16 milligrams of extractable hydrocarbons (saturates and aromatics) per 1 gram of TOC, and this value is often used to estimate petroleum source rock potential. According to Powell (1978), good source rock potential is indicated by hydrocarbon yields above 50 mg HC/g TOC, marginal by 30-50 mg HC/g TOC, and samples containing less than 30 mg HC/g TOC usually have no source rock potential. Furthermore, Powell (1978) showed that the percentage of hydrocarbons in extract is useful in estimating thermal maturity, with <25%, 25-40% and 40-60% ranges corresponding to low, marginal and "oil window" maturities. A hydrocarbon ratio of more than 60% indicates staining or contamination. According to these criteria the organic matter in the analyzed sample is not only immature with respect to hydrocarbon generation but also has no petroleum source rock potential.

The saturate fraction was analysed using gas chromatography (GC). A Varian 3800 FID gas chromatograph was used with 30m DB-1 column (30m x 0.25mm ID, 0.25 micrometers film thickness), helium used as carrier gas and siloxane gum used as the fixed phase, temperature programmed from 60ºC to 300ºC at 6ºC/min and then held for 30 min at 300ºC. The eluting compounds were detected and quantitatively determined using a hydrogen flame ionization detector. The overall distribution of n-paraffins was used to constrain interpretation of the character of the original biological input as well as the relative thermal maturity. The resulting saturate fraction gas chromatogram (Fig. 7) shows a bimodal distribution of normal alkanes, smooth in n-C13 to n-C21 range, and centered at n-C16, followed by an increasing profile with a minor odd to even carbon number preference in the n-C23 to n-C26 range, often interpreted as indicating low maturity. The >n-C27 range appears to be dominated by higher molecular-weight non-alkane compounds, likely terpanes. The acyclic isoprenoids can be easily identified, with an apparent predominance of pristane (Pr) over phytane (Ph) resulting in the Pr/Ph ratio of 3.26, and Pr/n-C17 and Ph/n-C18 ratios of 1.43 and 0.57 respectively. The high Pr/Ph ratio, typically used as an indicator of the redox conditions during the deposition of organic matter, appears consistent with the high amount of the dominantly oxidized coaly, terrestrial organic matter present in the sample. However, while this type of organic matter tends to show higher concentration of n-paraffins in the n-C25 to n-C35 range, the concentrations of n-C13 to n-C25 alkanes in a sample that is thermally immature could indicate some input or admixture of higher maturity fraction.

The hydrocarbons were also analyzed by gas chromatography-mass spectroscopy (GC-MS). An Agilent 6890 FID gas chromatograph equipped with a 30 m DB-1 column (dimethylpolysiloxane, 0.25mm ID) was used in both analyses, while Waters and HP 5973 mass spectrometers were used to analyze saturate and aromatic fraction, respectively, operating at 70 eV ionization voltage, 100 mA filament emission current, 280ºC interface temperature. The saturate fraction chromatograms display low concentrations of biomarkers commonly used in petroleum analyses, such as terpanes and steranes, which confirms overall low maturity of the organic matter. Similarly, the aromatic fraction shows immature distribution of triaromatic steroids (C21-C22 TAS present in higher concentration than C26-C28 TAS), although some of the other biomarkers ratios that are affected by thermal maturity, like metylphenantrene index and trimethylnaphthalene ratio suggest slightly higher maturity. The non-marine Hassel strata containing coal seams occur directly on the Precambrian basement and appear to have a limited surface exposure in the area (Pawlowski, 1979). Hence there not enough geological data to combine with the biomarker data to hypothesize if this slightly more mature component is native to the sample or migrated from other stratigraphic intervals.

TIME	COMPOUND NAME	AREA	HEIGHT
11.81	C13	189.32	89.48
13.96	C14	1124.21	546.67
16.02	C15	2198.49	961.08
17.98	C16	2626.43	1172.57
19.85	C17	2054.46	908.61
20.03	Pr	2940.44	973.76
21.62	C18	1593.83	674.74
21.85	Ph	902.16	273.13
23.32	C19	2059.90	611.56
24.93	C20	1309.58	538.53
26.48	C21	1014.40	447.39
27.96	C22	1326.93	547.43
29.38	C23	1681.18	716.04
30.75	C24	1567.51	644.67
32.06	C25	2813.12	1200.62
33.32	C26	1527.16	537.81
34.55	C27	1585.45	650.41
35.74	C28	4892.13	1525.90
36.86	C29	1796.58	406.64
37.96	C30	939.45	284.76
39.03	C31	746.49	237.00
40.05	C32	271.14	88.87

Table 1. Gas chromatogram values of sample collected from the Hassel Formation

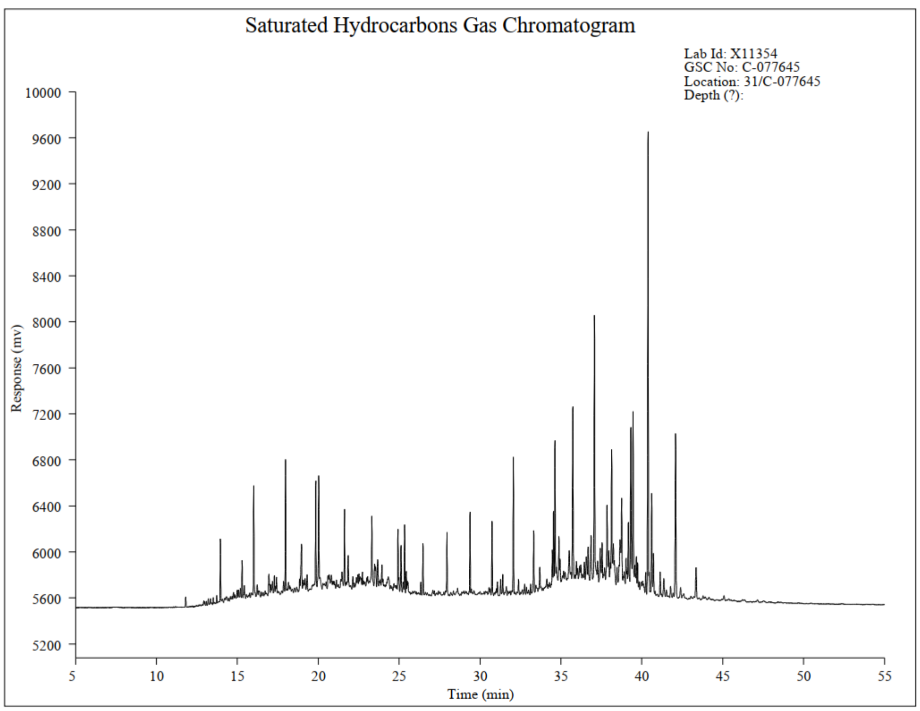

Figure 7. Saturate fraction gas chromatogram of sample collected from the Hassel Formation.

VITRINITE REFLECTANCE RESULTS

Vitrinite reflectance measurements were done on 50 points from each of 16 samples collected during the 2009 GSC fieldwork (Table 2). Figure 8 shows location of the 16 samples. Vitrinite reflectance (VRo%) varies between 0.27% and 0.49% with an average of 0.41%. Industry collected 27 samples ranging between 0.22% and 0.56% with an average of 0.36% (Cooper et al., 1976). The average of the total data set is 0.38 VRo% (Fig. 9).

Name	Ro	Sd	n	E	N	alt m
HFB09 13	0.39	0.033	50	589308	8091214	51
HFB09 21A	0.37	0.019	50	578567	8087210	123
HFB09 21B	0.42	0.036	50	578536	8087146	131
HFB09 23	0.35	0.050	50	586292	8046560	187
HFB09 24B	0.41	0.034	50	586466	8046438	
HFB09 25A	0.46	0.049	50	588223	8048839	197
HFB09 25C	0.42	0.035	50	588223	8048839	
HFB09 26	0.49	0.036	50	596355	8061038	37
HFB09 32	0.44	0.045	50	528134	8108861	-15
HFB09 37	0.27	0.035	50	566354	8161711	242
HFB09 40	0.44	0.045	50	538130	8128347	298
HFB09 66	0.42	0.039	50	510033	8141248	254
HFB09 82	0.46	0.024	50	568630	8078892	39
HFB09 86	0.46	0.065	28	560158	8094729	412
HFB09 88	0.38	0.045	50	583418	8092556	436
WIA09 12	0.42	0.050	50	532767	8125977	334

Table 2: Vitrinite reflectance results of 16 samples collected during the 2009 GSC fieldwork.

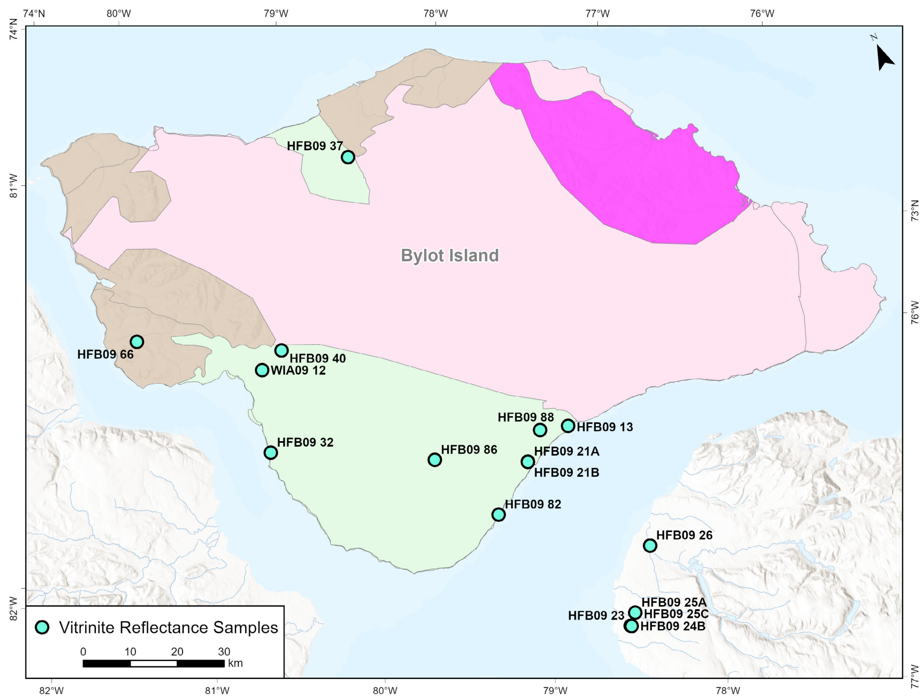

Figure 8. Vitrinite reflectance sample locations

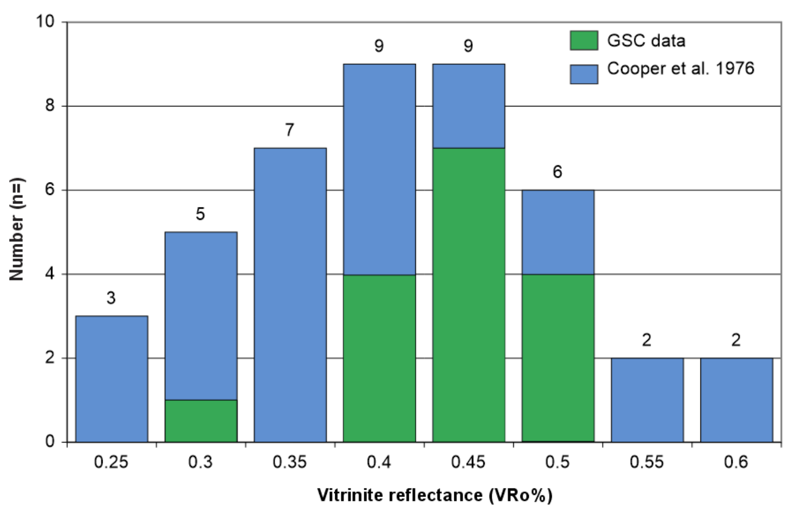

Figure 9. Vitrinite reflectance values measured by the GSC (green) and Industry (blue). The average of the dataset is 0.38 VRo%.

SOURCE ROCK QUALITY

Proterozoic samples have poor source rock potential given the very low S2 values. However, TOC is in the very good to excellent range indicating that these strata had an original source rock potential that must have been excellent, but no hydrocarbon generation (Fustic et al., 2017).

The source quality of the Cretaceous to Cenozoic succession is generally poor with 81% of the samples with S2 <2.5 mg HC/g rock, 11% have fair potential (19/137), 2% have good potential (4/167), 2% have very good potential (3/167) and 3% have excellent potential (5/167). Pseudo van Krevelen diagram indicates primarily Type III kerogen, which is derived from terrestrial plants and is gas prone.

THERMAL MATURITY

Proterozoic strata have a high thermal maturity, generally exceeding the calibration of the Rock-Eval instrument. Jarvie (2018) equates Tmax 480 °C to an equivalent vitrinite reflectance of 1.41% but the calibration between Tmax and VRo_equivalent above that temperature is poor.

Stolper et al., (2014) stated that oil that is not expelled is destroyed by conversion to pyrobitumen and gas by ~190 °C, with thermogenic gas generation taking place between 160 °C and 220 °C from oil- or gas-prone kerogen. Gas data from drill cuttings show a decrease in gas concentrations above VRo% of ~2.5%, which indicates that methane is expelled or destroyed faster than it is created at ~220 °C (Dewing et al., 2007b). Likely, the thermal maturity of Proterozoic strata exceeds the limit (190 °C) of oil preservation and may exceed the preservation limit (220 °C) of gas.

The thermal maturity of Cretaceous-Cenozoic strata as measured by vitrinite reflectance is about 0.4%, or below the onset of thermogenic hydrocarbon generation, which starts between 0.45% and 0.5% VRo. Average Tmax is 425 °C, which equates to an equivalent vitrinite reflectance of 0.49%, or near the onset of hydrocarbon generation. The higher apparent thermal maturity in the Rock-Eval data is probably due to recycled thermally mature organic matter in the rocks which is measured by the bulk Rock-Eval technique, but which would be avoided by an organic petrologist who only measures vitrinite particles.

CONCLUSION

The source rock quality and thermal maturity of samples from Bylot Island are quite low and in their current state, could not be the source of the natural oil seeps observed around the study area. The quality of these source rocks will need to improve offshore, to be correlated with the oil seeps observed in the area. There is also the possibility of other source rocks not observed on Bylot Island being responsible for the oil seeps.

ACKNOWLEDGEMENTS

The earliest version of this open file was written by Hans Wielens, who passed away before the paper could be published. Thanks to Chris Lister for the internal review of this open file, your suggestions contributed to the quality of the write up. Lisel Currie is thanked for her valuable input regarding Bylot Island geology. Thanks to Barbara Medioli and Sonya Dehler for program management.

REFERENCES

Bojesen-Koefoed, J.A., Christiansen, F.G., Nytoft, H.P., and Pedersen, A.K., 1999. Oil seepage onshore West Greenland: evidence of multiple source rocks and oil mixing. *In* Geological Society, London, Petroleum Geology Conference Series, vol. 5, no. 1, pp. 305-314.

Burden, E.T., and Langille, A.B., 1990. Stratigraphy and sedimentology of Cretaceous and Paleocene strata in half-grabens on the southeast coast of Baffin Island, Northwest Territories. Bulletin of Canadian Petroleum Geology, 38(2), p. 185-196.

Carey, J.S., McCartney, T., Hanna, M.C., Lister, C.J., and Kung, L.E., 2020. Qualitative petroleum resource assessment of the Labrador Margin. Geological Survey of Canada, Open File 8535, (ed. rev.), 104 p. https://doi.org/10.4095/326017

Cooper, B.S., Fisher, M.J., Simpson, W.B., Butterworth, J.S., 1976. Report on a source rock and maturity evaluation of field samples from Bylot Island, Northwest Territories, Canada. Robertson Research report 4017P. National Energy Board of Canada file 511-01-12-022.

Currie, L.D., Brent, T.A., and Turner, E.C., 2020. Offshore bedrock geology of Eclipse Sound and Pond Inlet: connecting the structure and stratigraphy of Bylot and northern Baffin islands. Canadian Journal of Earth Sciences. 57(10), p. 1254-1267. https://doi.org/10.1139/cjes-2019-0159

Decker, V., Budkewitsch, P., and Tang, W. 2013. Database of suspect oil seeps in the marine environment of Baffin Bay and Davis Strait, Nunavut, identified from a survey of RADARSAT-2 data. Geological Survey of Canada, Open File 7404, 12 p. https://doi.org/10.4095/292761

Dewing, K., Obermajer, M., and Snowdon, L.R., 2007b, Geological and geochemical data from the Canadian Arctic Islands, Part VII: Composition of gas from petroleum exploration borehole cuttings: Geological Survey of Canada Open File 5611.

Fustic, M., Ardakani, O.H., Jiang, C., Turner, E., Mort, A., Sanei, H., Gonzales, G., and Long, D., 2017. Preliminary petroleum potential and organic matter characterization of the Mesoproterozoic upper Arctic Bay Formation (Black Shale) at the Shale Valley Central, northern Baffin Island, Nunavut, Canada. Gussow Research Conference 2017, Lake Louise, Alberta, p. 8-11.

Haggart, J.W., Dafoe, L.T., Bell, K.M., Williams, G.L., Burden, E.T., Currie, L.D., Fensome, R.A., and Sweet, A.R., 2022. Historical development of a litho- and biostratigraphic framework for onshore Cretaceous-Paleocene deposits along western Baffin Bay. In, Geological synthesis of Baffin Island (Nunavut) and the Labrador-Baffin Seaway; Dafoe, L.T. and Bingham-Koslowski, N. (eds.) Geological Survey of Canada, Bulletin 608, p. 107-135, https://doi.org/10.4095/321828

Jackson, G.D., Davidson, A., and Morgan, W.C. 1975. Geology of the Pond Inlet map-area, Baffin Island, District of Franklin. Geological Survey of Canada, Paper 74-25, 33pp., 1 sheet.
Jackson G.D., and Davidson, A., 1975a. Bylot Island map-area, District of Franklin. Geological Survey of Canada, Paper 74-29, 12 p.

Jackson G.D., and Davidson, A., 1975b. Geology, Bylot Island, District of Franklin. Geological Survey of Canada, Map 1397A.

Jackson, G.D. and Sangster, D.F., 1987 Geology and Resource Potential of a Proposed National Park, Bylot Island and Northwest Baffin Island, Northwest Territories. Geological Survey of Canada, Paper 87-17, 31 p.

Jarvie, D., 2018. Correlation of Tmax and measured vitrinite reflectance. TCU Energy Institute, p. 1-13.

Miall, A.D., Balkwill, H.R., and Hopkins, W.S., 1980. Cretaceous and tertiary sediments of Eclipse Trough, Bylot Island area, Arctic Canada, and their regional setting. Geological Survey of Canada, Paper 79-23, 20 p.

Moir, P.N., Oakey, G.N., Bennett, R., Dickie, K., Williams, G., Budkewitsch, P., Decker, V., Fowler, M.G., Obermajer, M., and Haggart, J.W. 2012. Natural oil seeps on the Baffin Shelf, Nunavut, Canada: geology and geochemistry of the Scott Inlet seep. Geological Survey of Canada, Scientific Presentation 12, 1 sheet, https://doi.org/10.4095/291575

Oakey, G.N., Moir, P.N., Brent, T., Dickie, K., Jauer, C., Bennett, R., Williams, G., MacLean, B., Budkewitsch, P., Haggart, J. and Currie, L., 2012. The Scott Inlet–Buchan Gulf oil seeps: actively venting petroleum systems on the northern Baffin margin offshore Nunavut, Canada. Canadian Society of Petroleum Geologists, Annual Convention, Calgary, Alberta.
Turner, E.C., 2009. Mesoproterozoic carbonate systems in the Borden Basin, Nunavut. Canadian Journal of Earth Sciences v. 46(12), p. 915–938. doi: https://doi.org/10.1139/E09-062

Pawlowski, I.R. 1979. An investigation of coal exposures near Pond Inlet, Baffin Island. Indian and Northern Affairs Canada, Mineral Industry Repot EGS 1978-11, p. 136-138

Powell, T.G., 1978. An assessment of the hydrocarbon source rock potential of the Canadian Arctic Islands. Geological Survey of Canada, Paper 78-12, 82 pp.

Stolper, D.A., Lawson, M., Davis, C.L., Ferreira, A.A., Santos Neto, E.V., Ellis, G.S., Lewan, M.D., Martini, A.M., Tang, Y., Schoell, M., Sessions, A.L., and Eiler, J.M., 2014, Formation temperatures of thermogenic and biogenic methane: Science, v. 344, p. 1500–1503, https://doi.org/10.1126/science.1254509

Turner, E.C. 2009. Mesoproterozoic carbonate systems in the Borden Basin, Nunavut. Canadian Journal of Earth Sciences. 46. 915-938. 10.1139/E09-062.

Waterfield, J.J., 1989. Stratigraphy, sedimentology and palynology of Cretaceous and Tertiary strata, southwest Bylot Island, Northwest Territories, Canada. Unpublished MSc thesis, Memorial University of Newfoundland, 290 p.

APPENDIX A

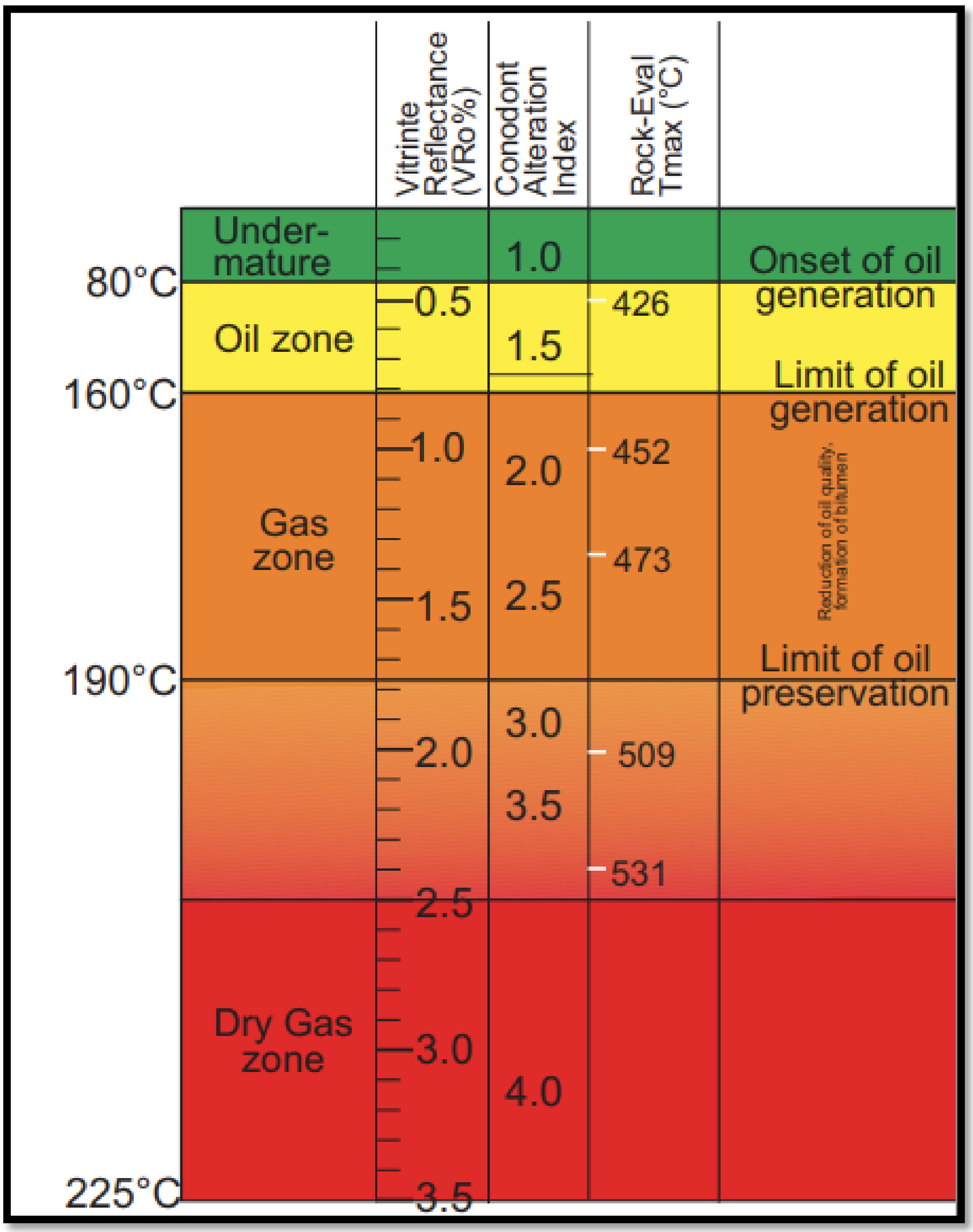

Figure A-1: Chart showing limit of Hydrocarbon generation and preservation. (Dewing et al, 2007b)

TABLE A-1: Results of Rock-Eval analysis of samples from Bylot Island.

Curation	Latitude	Longitude	Sample	Qty	S1	S2	S3	Tmax	TOC	PC(%)	RC%	HI	OI	MINC%	Age	Lithology
C-033863	73.6340474	-79.1325035	74-BAA-65A	70.2	0.07	2.86	5.86	432	4.26	0.52	3.74	67	138	1.14	Late Cretaceous	
C-033864	73.6340474	-79.1325035	74-BAA-65B	70.0	0.07	2.68	3.97	433	3.63	0.42	3.21	74	109	0.69	Late Cretaceous	
C-060107	73.2423526	-79.815903	77HFA41-7	20.7	0.4	15.66	11.59	410	14.63	2.3	12.33	107	79	0.68	upper Albian to Cenomanian	coal
C-060108	73.2423526	-79.815903	77HFA41-8	70.2	0.03	0.09	2.43	420	2.65	0.19	2.46	3	92	0.5	upper Albian to Cenomanian	
C-060109	73.2423526	-79.815903	77HFA41-9	10.6	0.79	30.51	20.43	415	35.54	4.44	31.1	86	57	1.71	upper Albian to Cenomanian	coal
C-060110	73.2423526	-79.815903	77HFA41-10	71.0	0.05	0.52	0.86	427	1.34	0.11	1.23	39	64	0.16	Campanian-Maastrichtian	
C-060111	73.2423526	-79.815903	77HFA41-11	70.4	0.05	0.35	0.45	413	0.8	0.07	0.73	44	56	0.12	Campanian-Maastrichtian	
C-060112	73.2423526	-79.815903	77HFA41-12	70.2	0.3	1.1	0.34	415	0.8	0.15	0.65	138	43	0.1	Campanian-Maastrichtian	
C-060113	73.2423526	-79.815903	77HFA41G-13	70.5	0.15	1.28	1.84	418	2.23	0.25	1.98	57	83	0.28	Campanian-Maastrichtian	
C-060116	73.1590191	-79.7075686	77HFA42A-16	70.4	0.01	0.16	0.76	438	0.5	0.05	0.45	32	152	0.07	upper Paleocene	
C-060117	73.1590191	-79.7075686	77HFA42-17	70.7	0.02	0.04	0.82	437	0.22	0.03	0.19	18	373	0.09	upper Paleocene	
C-060118	73.1590191	-79.7075686	77HFA42B-18	70.7	0.01	0.26	1.31	443	0.84	0.08	0.76	31	156	0.11	upper Paleocene	
C-060119	73.1590191	-79.7075686	77HFA42-19	70.6	0.01	0.38	1	436	0.94	0.09	0.85	40	106	0.12	upper Paleocene	
C-060120	73.1590191	-79.7075686	77HFA42-20	70.1	0.06	0.7	2.72	438	1.94	0.19	1.75	36	140	0.3	upper Paleocene	
C-060121	73.1590191	-79.7075686	77HFA42-21	70.6	0.04	1.21	1.69	438	2.53	0.21	2.32	48	67	0.22	upper Paleocene	
C-060122	73.1590191	-79.7075686	77HFA42-22	70.5	0.09	0.85	1.86	433	1.95	0.17	1.78	44	95	0.25	upper Paleocene	
C-060123	73.1590191	-79.7075686	77HFA42-23	70.9	0.15	0.42	1.19	418	1.31	0.14	1.17	32	91	0.21	upper Paleocene	
C-060124	73.2173516	-79.8825766	77HFA44-24	70.7	0.15	0.74	2.97	428	1.63	0.19	1.44	45	182	0.38	upper Paleocene	
C-060126	73.2173516	-79.8825766	77HFA44-26	70.7	0.07	1.07	1.45	427	2.14	0.2	1.94	50	68	0.17	upper Paleocene	
C-060127	73.2173516	-79.8825766	77HFA44-27	70.5	0.13	0.79	0.93	429	1.56	0.15	1.41	51	60	0.26	upper Paleocene	

C-060128	72.7173529	-78.2658066	77HFA46A-28	70.7	0.03	0.2	2.93	421	2.91	0.2	2.71	7	101	0.3	upper Albian to Cenomanian	sandstone
C-060129	72.7256866	-78.2658062	77HFA46A-29	70.3	0.39	7.11	3.34	415	4.5	0.86	3.64	158	74	0.35	Campanian-Maastrichtian	
C-076003	73.2423526	-79.815903	77BAA41C	70.9	0.02	0.07	0.15	399	0.08	0.02	0.06	88	188	0.03	Cretaceous	basal sandstone
C-076004	73.2423526	-79.815903	77BAA41D	70.4	0.04	0.63	0.66	422	1.43	0.11	1.32	44	46	0.15	Cretaceous	basal sandstone
C-076005	73.2423526	-79.815903	77BAA41E	70.9	0.07	0.35	0.51	429	0.49	0.06	0.43	71	104	0.9	Cretaceous	glauconitic sandstone
C-076006	73.2423526	-79.815903	77BAA41F	70.8	0.05	0.56	0.85	418	0.98	0.12	0.86	57	87	0.18	Cretaceous	lower shale
C-076007	73.2423526	-79.815903	77BAA41G	70.0	0.22	2.26	0.96	423	1.92	0.27	1.65	118	50	0.26	Cretaceous	lower shale
C-076009	73.1590191	-79.7075686	77BAA42A	70.2	0.12	2.16	1.22	427	1.96	0.27	1.69	110	62	0.26	Cretaceous - Tertiary	brown sandstone
C-076010	73.1590191	-79.7075686	77BAA42B	70.6	0.02	0.07	0.22	401	0.06	0.02	0.04	117	367	0.04	Cretaceous	second sandstone
C-076011	73.2173516	-79.8825766	77BAA44A	70.4	0.01	0.03	0.15	380	0.06	0.01	0.05	50	250	0.01		
C-076012	73.2173516	-79.8825766	77BAA44B	70.9	0.04	0.46	1.33	423	1.35	0.12	1.23	34	99	0.16	upper Paleocene	
C-076013	73.6840466	-79.7492208	77BAA45A	70.4	0.1	0.29	0.2	436	0.2	0.06	0.14	145	100	12.24	Proterozoic ?	
C-076014	73.6840466	-79.7492208	77BAA45B	70.6	0.02	0.05	0.18	381	0.14	0.01	0.13	36	129	3.22	Proterozoic ?	
C-076015	73.6840466	-79.7492208	77BAA45C	70.3	0.02	0.07	0.15	436	0.32	0.02	0.3	22	47	0.09	Proterozoic ?	
C-076016	73.6840466	-79.7492208	77BAA45D	70.0	0.08	0.38	0.35	421	0.76	0.07	0.69	50	46	0.09	Cretaceous ?	
C-077604	73.38403	-80.6826364	78-MLA-3-1	71.0	0.02	0.31	0.62	419	1.17	0.08	1.09	26	53	0.14		
C-077605	73.38403	-80.6826364	78-MLA-3-2	70.2	0.02	0.2	0.51	425	0.63	0.06	0.57	32	81	0.1		
C-077606	73.3839967	-80.6826031	3-3/C-077606	70.1	0.11	0.37	0.37	423	0.74	0.07	0.67	50	50	0.47		
C-077620	73.2006844	-79.8992456	9/C-077620-183	70.9	0.18	0.44	1.32	423	1.71	0.15	1.56	26	77	0.27		
C-077622	72.800689	-78.8658877	10-1/C-077622	70.7	0.02	0.05	0.1	424	0.06	0.01	0.05	83	167	0.04		
C-077623	72.800689	-78.8658877	10-2/C-077623	70.0	0.02	0.06	0.14	406	0.09	0.02	0.07	67	156	0.04		
C-077624	72.7839893	-79.1825213	11-1/C-077624	69.9	0.04	0.2	0.16	411	0.19	0.04	0.15	105	84	0.05		
C-077625	73.0506784	-80.1659742	12-1/C-077625	70.4	0.05	0.13	0.13	449	0.06	0.02	0.04	217	217	0.03		
C-077626	72.9673913	-78.8991834	13-1/C-077626	70	0.43	0.73	0.67	292	0.25	0.13	0.12	292	268	0.04	Kanguk Fm	
C-077627	72.9173926	-78.2824321	14-1/C-077627	70	0.01	0.08	0.24	433	0.08	0.02	0.06	100	300	0.03		
C-077628	72.9006921	-78.3824414	15-1/C-077628	71.1	0.01	0.02	0.13	313	0.02	0.01	0.01	100	650	0.04		
C-077629	72.8673909	-78.58246	16-1/C-077629	70	0.07	0.35	0.79	423	1.34	0.11	1.23	26	59	0.15		

C-077630	72.8673909	-78.58246	16-2/C-077630	70	0.01	0.02	0.1	389	0.03	0.01	0.02	67	333	0.04		
C-077631	72.9006921	-78.3991428	17-1/C-077631	70.8	0.03	0.06	0.17	321	0.06	0.02	0.04	100	283	0.04		
C-077632	72.8839917	-78.4158451	18-1/C-077632	70.6	0.03	0.09	0.43	344	0.07	0.03	0.04	129	614	2.57		
C-077633	72.8839916	-78.4491479	19-1/C-077633	70.2	0.03	0.06	0.22	311	0.07	0.03	0.04	86	314	0.08		
C-077634	72.9839911	-78.9824897	21-1/C-077634	70.8	0.01	0.05	0.39	386	0.05	0.02	0.03	100	780	0.25		
C-077635	73.2006846	-79.8492417	22-1/C-077635-70	70	0.05	0.14	0.48	405	0.1	0.04	0.06	140	480	0.06		
C-077636	73.283989	-80.282574	23-1/C-077636	70.6	0.04	0.21	0.59	301	0.18	0.04	0.14	117	328	3.48		
C-077637	73.283989	-80.282574	23-2/C-077637	50.6	0.2	4.95	6.15	419	16.93	1.02	15.91	29	36	0.77		
C-077638	72.9006918	-78.5991601	25-1/C-077638	70.5	0.02	0.3	0.57	420	0.61	0.07	0.54	49	93	0.17		
C-077639	72.9006909	-78.9324895	27-1/C-077639	70.6	0.01	0.04	0.14	400	0.1	0.02	0.08	40	140	0.03		
C-077640	73.6007133	-79.0491654	28-1/C-077640	70.1	0.01	0.05	0.2	432	0.05	0.02	0.03	100	400	0.04		
C-077641	73.634014	-79.1658729	29-1/C-077641	70.2	0.02	0.13	0.17	610	0.08	0.02	0.06	163	213	0.04		
C-077642	73.634014	-79.1658729	29-2/C-077642	70.7	0.04	0.93	1.1	433	1.64	0.17	1.47	57	67	0.2		
C-077643	72.6173812	-78.082431	31-1/C-077643	70.6	0.01	0.05	0.08	410	0.04	0.01	0.03	125	200	0.03		
C-077645	72.6173479	-78.0824643	31-3/C-077645	50.5	1.26	36.7	17.9	414	35.07	4.67	30.4	105	51	4.88	Hassel Fm	coal
C-077645	72.6173479	-78.0824643	31-3/C-077645	20.8	1.43	39.32	17.95	413	39.77	5.04	34.73	99	45	1.48	Hassel Fm	coal
C-077646	72.7006828	-77.7157968	32/C-077646	69.8	0.01	0.05	0.11	403	0.07	0.02	0.05	71	157	0.02		
C-077647	73.0673784	-79.8659489	33-1/C-077647	70.7	0.01	0.69	0.74	440	1.1	0.11	0.99	63	67	0.09		
C-077648	73.0673784	-79.8659489	33-2/C-077648	70.1	0.05	0.19	0.27	410	0.1	0.03	0.07	190	270	0.03		
C-077649	73.0339784	-79.8992549	34-1/C-077649	70.1	0.1	4.04	3.34	430	3.76	0.53	3.23	107	89	0.54		
V-000648	72.898758	-78.278186	WIA09-13	70.4	0.02	0.46	2.36	424	3.95	0.18	3.77	12	60	0.3		shale
V-000649	72.898232	-78.281774	WIA09-14-B	69.7	0.04	1.57	1.00	421	1.96	0.2	1.76	80	51	0.1		shale
V-000650	72.898232	-78.281774	WIA09-14-C	70.6	0.02	0.09	0.25	432	0.18	0.02	0.16	50	139	10.9		shale
V-000651	72.883342	-78.44128	WIA09-19-A	70.3	0.03	1.26	1.13	420	1.80	0.17	1.63	70	63	0.2		shale
V-000652	72.883342	-78.44128	WIA09-19-B	70.8	0.02	0.92	1.14	416	1.60	0.14	1.46	58	71	0.2		shale
V-000653	72.883342	-78.44128	WIA09-19-C	70.2	0.02	1.39	1.22	422	1.75	0.18	1.57	79	70	0.1		shale
V-000654	72.883617	-78.449557	WIA09-20	70.3	0.03	1.51	1.60	421	1.88	0.21	1.67	80	85	0.2		shale
V-000655	72.867004	-78.610009	WIA09-21-A	70.6	0.00	0.23	1.23	431	1.26	0.08	1.18	18	98	0.1		shale
V-000656	72.866442	-78.611029	WIA09-21-B	70.2	0.02	1.58	1.80	427	2.73	0.23	2.50	58	66	0.2		coal
V-000657	72.500071	-78.428265	WIA09-23	10.3	0.14	9.84	49.26	413	45.95	3.30	42.65	21	107	2.0		shale
V-000657	72.500071	-78.428265	WIA09-23	10.8	0.18	8.19	53.85	411	46.14	3.33	42.81	18	117	2.2		shale

V-000658	72.498911	-78.423242	WIA09-24-A	70.2	0.12	2.50	16.77	417	11.30	0.91	10.39	22	148	0.8		shale
V-000659	72.519731	-78.367818	WIA09-25-D	70.7	0.03	2.55	1.50	414	2.46	0.29	2.17	104	61	0.1		shale
V-000660	73.073309	-80.134236	WIA09-32	70.6	0.04	5.49	0.80	423	3.16	0.51	2.65	174	25	0.2		shale
V-000663	73.617522	-79.202282	WIA09-35-A	70.5	0.03	3.12	5.18	426	4.80	0.48	4.32	65	108	1.3		shale
V-000664	73.617522	-79.202282	WIA09-35-B	70.7	0.03	3.53	4.30	429	4.46	0.47	3.99	79	96	0.6		shale
V-000665	73.617522	-79.202282	WIA09-35-C	70.6	0.02	1.52	4.94	429	2.77	0.43	2.34	55	178	5.7		shale
V-000666	73.617522	-79.202282	WIA09-35-E	70.0	0.01	0.12	5.52	418	0.52	0.17	0.35	23	1062	0.6		shale
V-000667	73.617522	-79.202282	WIA09-35-F	70.4	0.01	0.81	2.51	430	1.40	0.26	1.14	58	179	6.7		shale
V-000668	73.617522	-79.202282	WIA09-35-G	70.0	0.02	3.70	4.62	432	5.44	0.49	4.95	68	85	0.4		shale
V-000669	73.621312	-79.205056	WIA09-36	70.4	0.03	3.82	1.85	430	4.73	0.43	4.30	81	39	0.3		shale
V-000670	73.246508	-79.818743	WIA09-41-A	70.7	0.01	0.54	0.66	427	1.42	0.08	1.34	38	46	0.1		shale
V-000671	73.246508	-79.818743	WIA09-41-B	70.3	0.01	0.30	0.64	428	1.07	0.06	1.01	28	60	0.1		shale
V-000672	73.246508	-79.818743	WIA09-41-C	70.4	0.01	0.69	0.48	429	1.38	0.08	1.30	50	35	0.1		shale
V-000673	73.246508	-79.818743	WIA09-42-B	70.3	0.01	0.66	0.24	432	1.25	0.07	1.18	53	19	0.1		shale
V-000674	73.246508	-79.818743	WIA09-42-C	70.5	0.01	0.38	0.25	431	0.65	0.05	0.60	58	38	0.1		shale
V-000675	73.245878	-79.821367	WIA09-43	70.4	0.01	0.33	0.48	430	1.01	0.05	0.96	33	48	0.1		shale
V-000676	73.246878	-79.830189	WIA09-44-A1	70.7	0.03	2.81	1.65	419	2.59	0.32	2.27	108	64	0.1		shale
V-000677	73.246878	-79.830189	WIA09-44-A2	70.5	0.03	2.19	1.24	418	1.84	0.24	1.60	119	67	0.1		shale
V-000678	73.246878	-79.830189	WIA09-44-B	70.1	0.13	13.28	2.32	413	4.59	1.24	3.35	289	51	0.2		shale
V-000679	73.245048	-79.828324	WIA09-45	70.6	0.01	0.47	0.38	418	0.71	0.06	0.65	66	54	0.0		shale
V-000680	73.244451	-79.827556	WIA09-46	70.4	0.01	0.39	0.43	418	0.73	0.06	0.67	53	59	0.1		shale
V-000681	73.244229	-79.829405	WIA09-47-A	70.5	0.01	0.52	0.19	418	0.70	0.06	0.64	74	27	0.1		shale
V-000682	73.242993	-79.831229	WIA09-49	70.3	0.02	0.86	0.22	414	0.94	0.09	0.85	91	23	0.1		shale
V-000683	73.242897	-79.831795	WIA09-50	70.7	0.02	0.94	0.20	423	0.98	0.10	0.88	96	20	0.2		shale
V-000684	73.241921	-79.833602	WIA09-52-B	70.2	0.03	1.65	0.31	423	1.32	0.16	1.16	125	23	0.2		shale
V-000685	73.24221	-79.833924	WIA09-52-D	70.4	0.03	1.54	0.41	424	1.40	0.16	1.24	110	29	0.2		shale
V-000686	73.241884	-79.835003	WIA09-53-A	70.5	0.02	2.38	0.38	427	1.79	0.23	1.56	133	21	0.2		shale
V-000687	73.242065	-79.835177	WIA09-53-B	70.1	0.03	2.29	0.39	427	1.71	0.22	1.49	134	23	0.4		shale
V-000688	73.239345	-79.837784	WIA09-54-A	70.8	0.01	0.49	0.61	427	0.93	0.23	0.70	53	66	2.1		shale
V-000689	73.239345	-79.837784	WIA09-54-B	70.4	0.02	1.77	0.39	429	1.55	0.18	1.37	114	25	0.2		shale
V-000690	73.237466	-79.838439	WIA09-55	70.6	0.01	1.30	0.42	428	1.40	0.13	1.27	93	30	0.2		shale

V-000691	73.237466	-79.838439	WIA09-56	70.1	0.01	1.30	0.38	429	1.46	0.13	1.33	89	26	0.2		shale
V-000692	73.236875	-79.838696	WIA09-57-A	69.9	0.03	3.67	0.75	423	2.60	0.36	2.24	141	29	0.3		shale
V-000693	73.236875	-79.838696	WIA09-57-B	70.4	0.02	2.41	0.43	428	2.12	0.23	1.89	114	20	0.3		shale
V-000694	73.236875	-79.838696	WIA09-57-C	70.5	0.02	4.31	0.61	422	2.60	0.40	2.20	166	23	0.1		shale
V-000695	73.234131	-79.835339	WIA09-58	70.6	0.01	0.65	0.51	424	1.45	0.09	1.36	45	35	0.4		shale
V-000696	73.232802	-79.833317	WIA09-60	70.9	0.01	0.66	0.34	425	1.33	0.08	1.25	50	26	0.3		shale
V-000697	73.2067	-79.662447	WIA09-61	70.2	0.01	0.46	1.00	424	1.63	0.10	1.53	28	61	0.1		shale
V-000698	73.242686	-80.322052	WIA09-64-B	70.3	0.01	0.68	0.60	422	1.69	0.09	1.60	40	36	0.1		shale
V-000700	73.374929	-80.68182	WIA09-67-A	70.8	0.02	1.27	0.79	421	2.08	0.16	1.92	61	38	0.1		shale
V-000701	73.374929	-80.68182	WIA09-67-B	70.4	0.00	0.74	0.31	432	1.23	0.08	1.15	60	25	0.1		shale
V-000702	73.374929	-80.68182	WIA09-67-C	70.8	0.00	0.35	0.17	431	0.68	0.04	0.64	51	25	0.1		shale
V-000703	73.374929	-80.68182	WIA09-67-D	70.7	0.01	0.42	0.21	431	0.89	0.05	0.84	47	24	0.1		shale
V-000704	73.235143	-79.999977	WIA09-69	70.6	0.01	2.83	0.27	425	1.70	0.26	1.44	166	16	0.2		shale
V-000705	73.224546	-79.983391	WIA09-72	70.6	0.01	0.99	0.90	431	1.85	0.13	1.72	54	49	0.2		shale
V-000706	73.224546	-79.983391	WIA09-74	70.9	0.01	1.88	2.87	433	4.25	0.29	3.96	44	68	0.3		shale
V-000707	72.855487	-78.59569	WIA09-80	70.9	0.01	0.28	0.46	430	1.08	0.05	1.03	26	43	0.1		shale
V-000708	72.845559	-78.651147	WIA09-81	70.3	0.01	0.38	0.85	430	1.50	0.08	1.42	25	57	0.1		shale
V-000709	72.795812	-78.920787	WIA09-82	70.4	0.01	0.97	0.83	436	2.08	0.13	1.95	47	40	0.1		coal
V-000709	72.795812	-78.920787	WIA09-82	70.4	0.01	0.94	0.86	435	2.08	0.13	1.95	45	41	0.1		coal
V-000710	72.758538	-79.417328	WIA09-83	70.5	0.01	2.63	0.94	433	2.69	0.27	2.42	98	35	0.3		shale
V-000711	72.915212	-79.21192	WIA09-85	70.4	0.00	0.02	0.31	432	0.15	0.01	0.14	13	207	0.0		shale
V-000712	72.94018	-79.162577	WIA09-86	70.4	0.02	1.88	1.74	433	2.64	0.24	2.40	71	66	0.2		coal
V-000713	72.913095	-78.455725	WIA09-88	70.4	0.21	0.17	2.26	414	2.42	0.14	2.28	7	93	0.3		coal
V-000714	72.911604	-78.454171	WIA09-89	70.2	0.03	1.47	1.00	423	2.04	0.18	1.86	72	49	0.1		shale
V-000715	73.136558	-79.476503	WIA09-92	70.8	0.00	0.27	0.51	435	0.77	0.05	0.72	35	66	0.1		shale
V-000716	73.111343	-79.795936	WIA09-93	70.6	0.04	0.58	0.52	439	1.28	0.08	1.20	45	41	0.1		shale
V-000717	73.079744	-79.606697	WIA09-94	70.5	0.04	4.23	1.47	430	3.51	0.43	3.08	121	42	0.6		shale
V-000718	73.039889	-79.877408	WIA09-95	70.5	0.02	3.06	0.90	432	3.10	0.31	2.79	99	29	0.3		shale
V-000719	72.977776	-80.037945	WIA09-97	70.0	0.03	3.53	3.65	429	3.93	0.45	3.48	90	93	1.0		shale
V-000720	72.872862	-79.889975	WIA09-99-A	70.3	0.02	2.76	2.29	428	3.10	0.34	2.76	89	74	0.8		shale
V-000721	72.872862	-79.889975	WIA09-99-B	70.5	0.01	0.89	1.44	426	1.06	0.18	0.88	84	136	8.3		shale

V-000722	73.293228	-80.077359	WIA09-100	70.5	0.02	1.79	1.35	422	3.69	0.24	3.45	49	37	0.2		shale
	72.88	79.68	110703	70.6	0.02	0.07	0.20	418	0.05	0.02	0.03	140	400	1.9		
	72.88	79.68	210701	70.4	0.01	0.13	0.38	417	0.44	0.04	0.40	30	86	0.1		
	72.88	79.68	210702	70.6	0.01	0.15	0.61	418	0.70	0.06	0.64	21	87	0.2		
	72.88	79.68	210705	70.1	0.03	0.15	0.79	415	0.60	0.07	0.53	25	132	0.2		
	73.17	79.75	310710	70.3	0.01	0.65	1.80	440	1.74	0.13	1.61	37	103	0.2		
	73.233	79.83	260703	70.4	0.02	0.33	0.98	419	1.74	0.11	1.63	19	56	0.2		
	73.233	79.83	260701	70.6	0.03	0.73	1.09	414	2.17	0.16	2.01	34	50	0.2		
	73.233	79.83	260706	70.7	0.03	0.89	0.97	429	1.82	0.15	1.67	49	53	0.3		
	73.233	79.83	260709	70.4	0.02	0.55	1.21	431	1.46	0.11	1.35	38	83	0.2		
	72.88	79.68	210707	70.0	0.07	0.49	0.93	416	0.94	0.11	0.83	52	99	0.2		
	n/d	n/d	EB g1-1	70.6	0.04	0.07	3.13	424	5.29	0.18	5.11	1	59	0.5		
	n/d	n/d	3000701	70.0	0.02	0.63	1.73	427	1.72	0.14	1.58	37	101	0.2		
	n/d	n/d	PB 84	70.4	0.45	1.28	0.82	465	2.43	0.17	2.26	53	34	0.3		
	n/d	n/d	PB 12	70.6	0.02	0.83	2.18	433	2.20	0.19	2.01	38	99	0.3		
	n/d	n/d	EB g1-02	20.5	0.39	20.36	16.43	411	20.76	2.92	17.84	98	79	0.9		
	n/d	n/d	EB 107	70.4	0.01	0.30	1.48	426	1.07	0.10	0.97	28	138	0.2		
	n/d	n/d	EB 105	70.3	0.01	0.91	1.08	433	1.70	0.13	1.57	54	64	0.2		
	n/d	n/d	PB 85	70.6	0.10	2.43	0.31	444	2.74	0.23	2.51	89	11	0.1		
	n/d	n/d	PB 6/2g-6	70.5	0.04	1.75	6.96	432	4.32	0.41	3.91	41	161	0.5		
	n/d	n/d	166	70.3	0.02	1.55	2.89	430	3.36	0.25	3.11	46	86	0.3		
	73.233	79.83	260701	70.3	0.03	0.54	1.43	414	1.93	0.13	1.80	28	74	0.3		
	n/d	n/d	Q 81	10.8	1.01	42.38	18.96	413	43.31	5.26	38.05	98	44	1.9		
	n/d	n/d	PB 6/2g-10	70.7	0.18	1.10	3.82	440	3.07	0.29	2.78	36	124	0.4		
	n/d	n/d	HW	10.6	0.46	11.19	28.44	421	52.78	3.06	49.72	21	54	2.6		
C-077369	74.7007991	-83.4162112	78 MSA-TG-8 243	70.1	0.02	0.07	0.22	441	0.05	0.02	0.03	140	440	11.81	Late Ordovician	
C-077371	74.7007991	-83.4162112	78 MSA-TG-8 249.9	70.1	0.01	0.05	0.19	448	0.05	0.01	0.04	100	380	11.53	Middle Ordovician	

APPENDIX B

Gas Chromatography - Mass Spectrometry Report
Organic Geochemistry Laboratory, Geological Survey of Canada - Calgary

Database Reference: Gas Chromatography - Mass Spectrometry Data for Crude Oils, Condensates and Rock Extracts, Geoscience Data Repository, Lands and Minerals Sector, Natural Resources Canada

Sample ID: X11354
GSC Catalog No: C-077645
Acquisition Date: 2012-09-06
Location: 31/C-077645 Upper Depth (?): Lower Depth (?):
Fraction: aromatic
Instrument: HP 6890 GC/HP 5973 MSD
MS Mode: Selected Ion Monitoring + EI
Temp Program: 100ºC 2 min hold, 40ºC/min to 180ºC, 4ºC/min to 320ºC 7 min hold
Column: DB-5ms, 30m x 0.32mm ID, 0.25 micrometers film thickness
Injection: split
Data Processing Software: MSD ChemStation E.02.00

Time	Compound Name	Area	Ion
13.87	137-TMN	91786	170
14.10	136-TMN	148850	170
14.54	135+146-TMN	95285	170
14.71	236-TMN	109858	170
15.87	125-TMN	257055	170
22.25	PH	183746	178
25.98	3-MPH	26898	192
26.16	2-MPH	37499	192
26.68	9-MPH	32883	192
26.88	1-MPH	28014	192
24.60	4-MDBT	15398	198
25.29	2+3-MDBT	3924	198
25.90	1-MDBT	13853	198
41.36	C20-TAS	39695	231
44.05	C21-TAS	10558	231
52.96	C26S-TAS	11042	231
54.84	C26R+C27S-TAS	26339	231
56.05	C28S-TAS	39181	231
56.69	C27R-TAS	22116	231
58.28	C28R-TAS	59765	231

Table B-1. Showing gas chromatography values of sample X11354 acquired in 2012

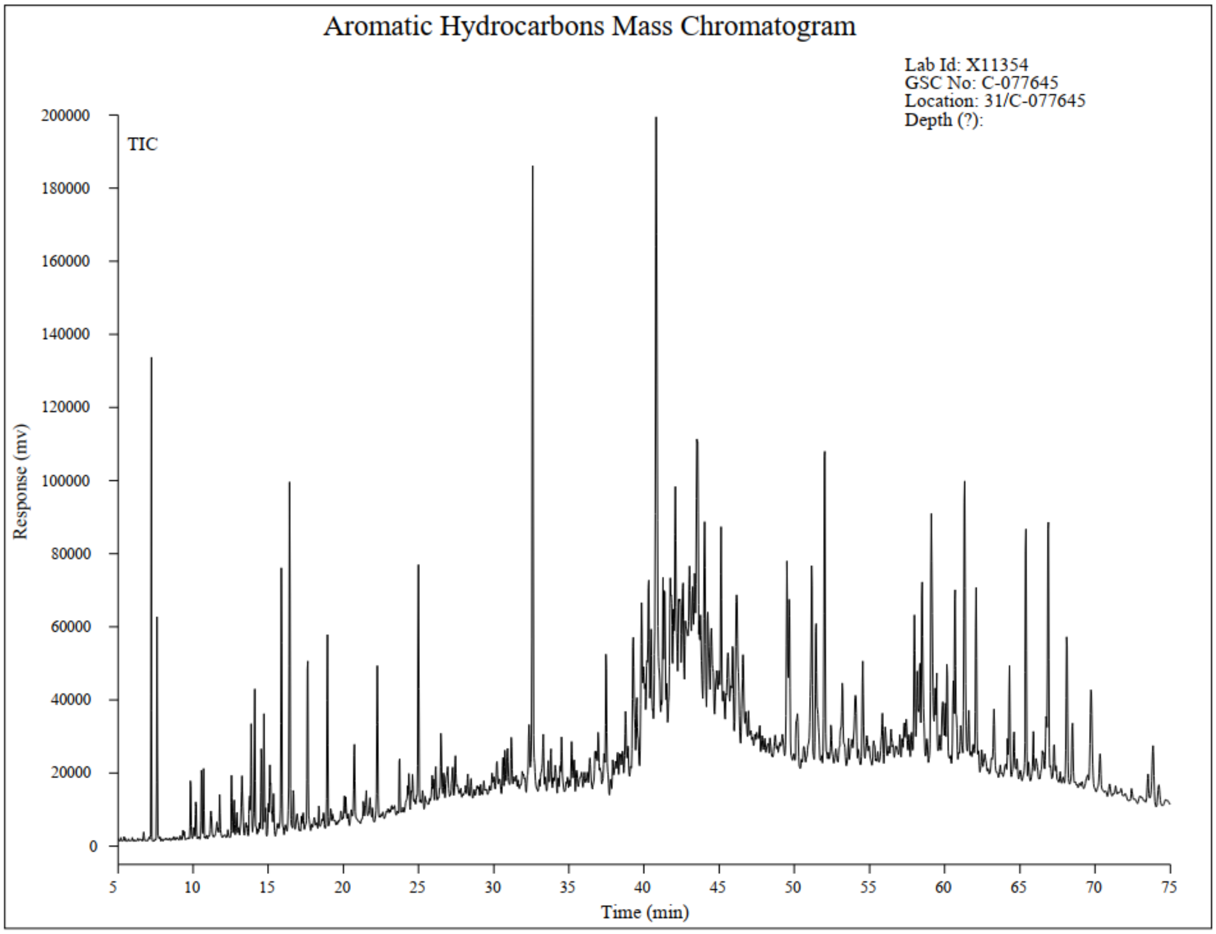

Figure B-1: Aromatic Hydrocarbons Mass Chromatogram

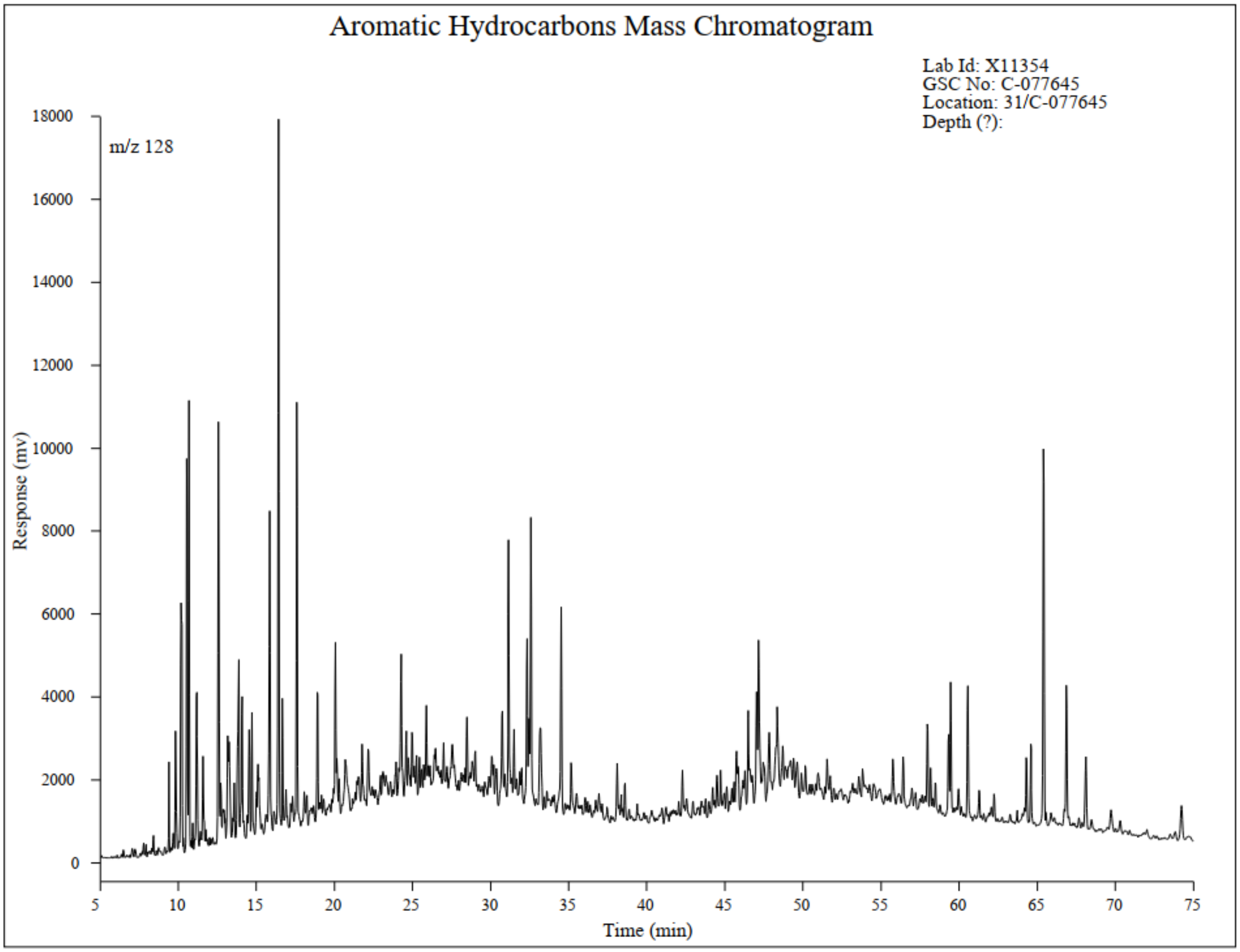

Figure B-2: Aromatic Hydrocarbons Mass Chromatogram

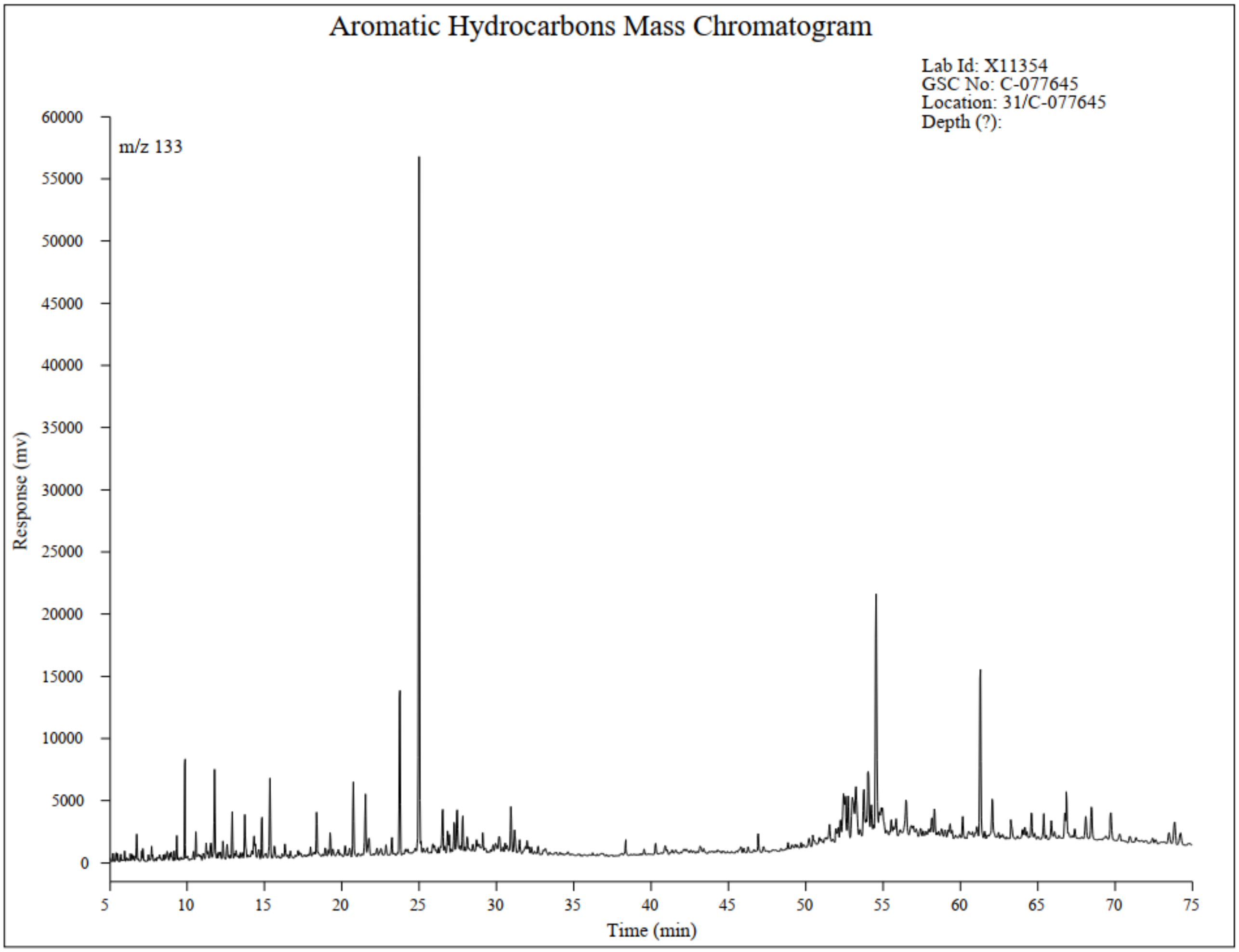

Figure B-3: Aromatic Hydrocarbons Mass Chromatogram

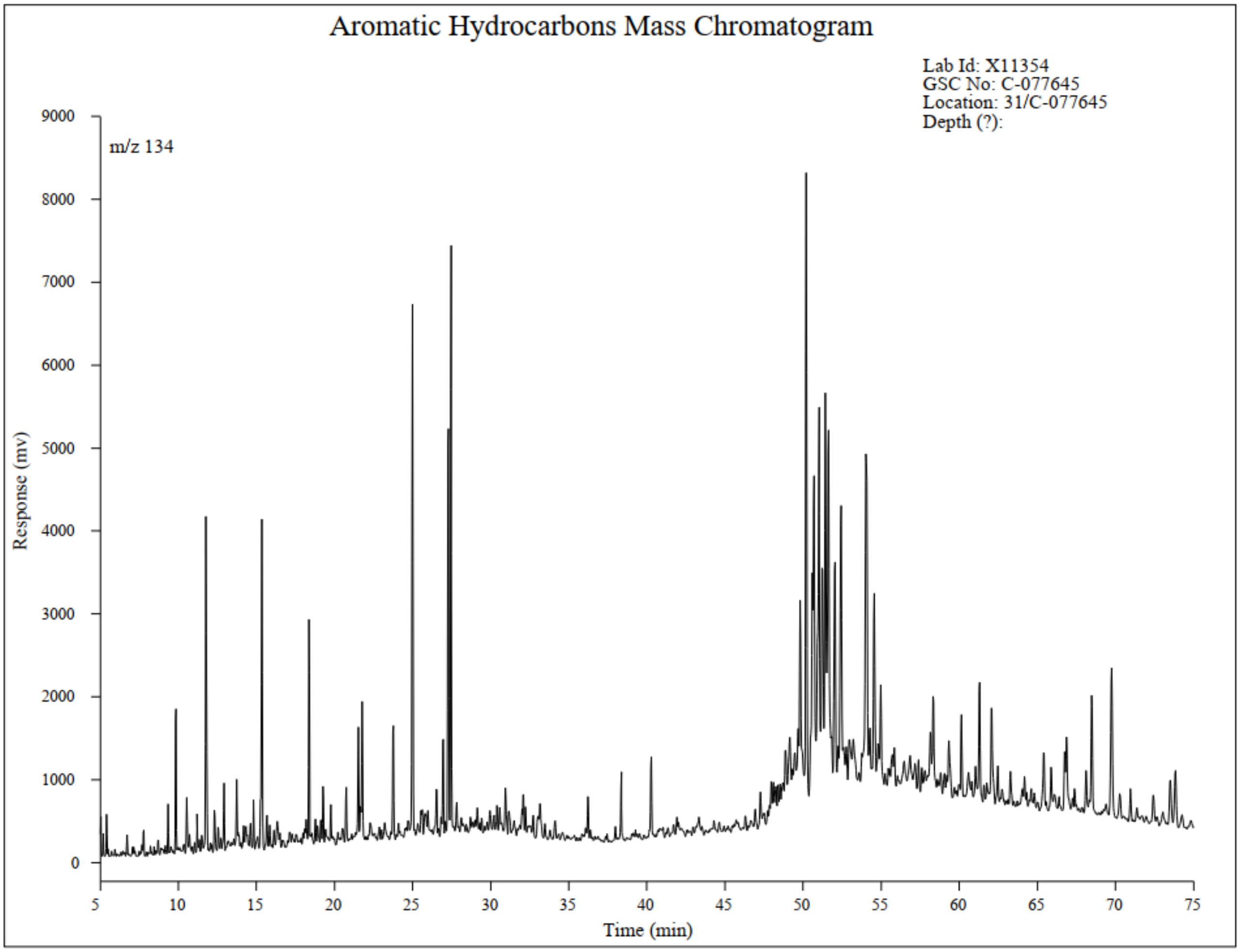

Figure B-4: Aromatic Hydrocarbons Mass Chromatogram

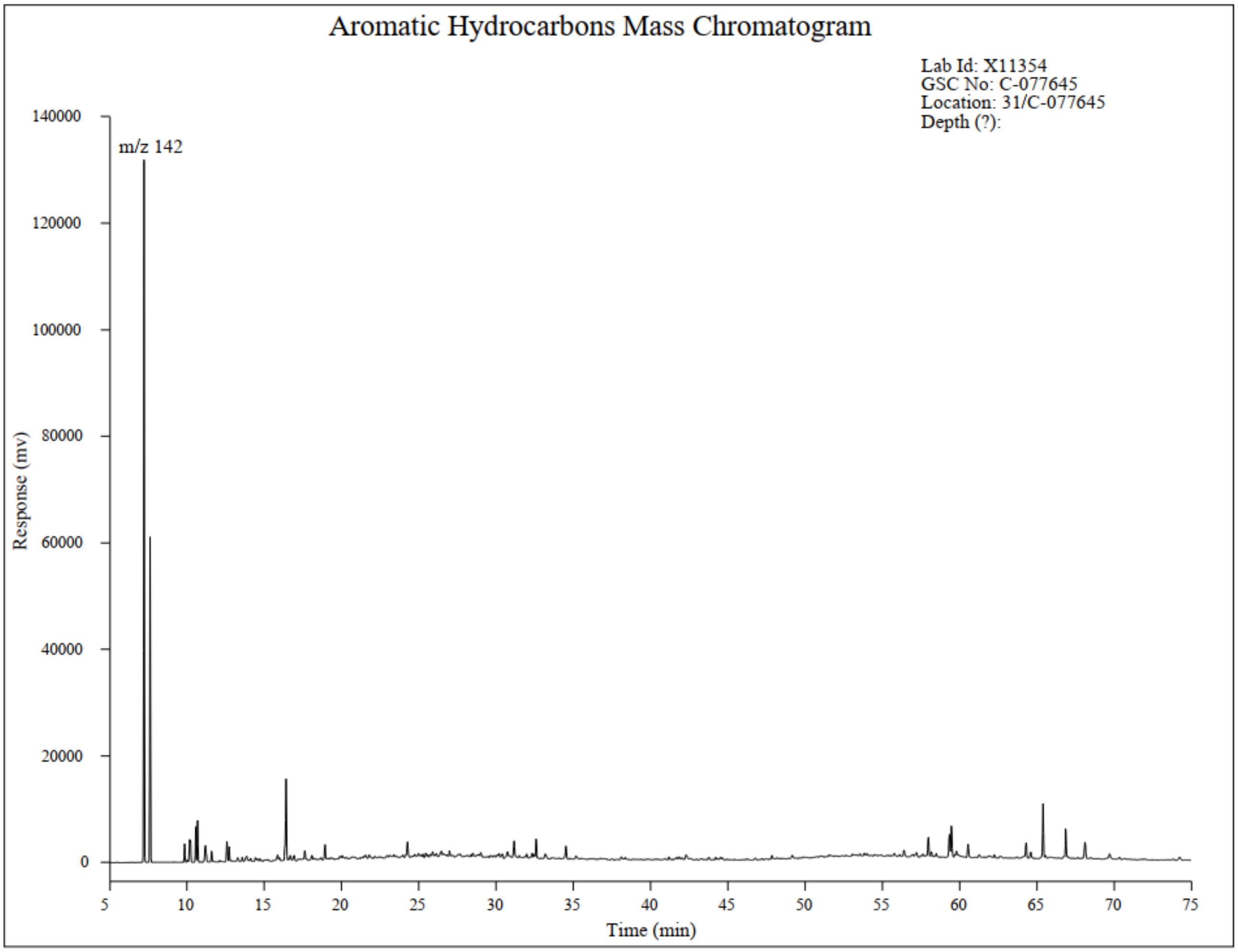

Figure B-5: Aromatic Hydrocarbons Mass Chromatogram

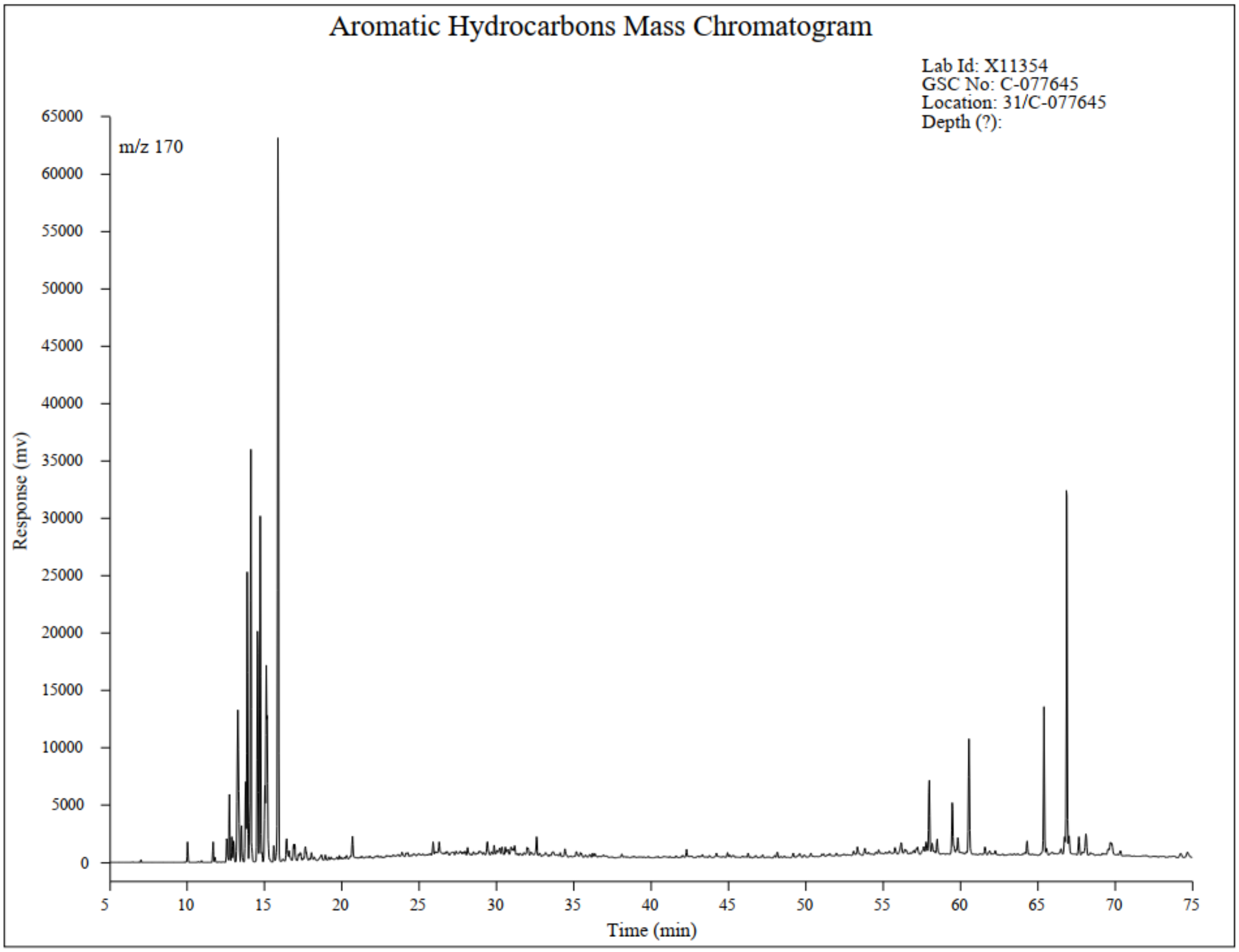

Figure B-6: Aromatic Hydrocarbons Mass Chromatogram

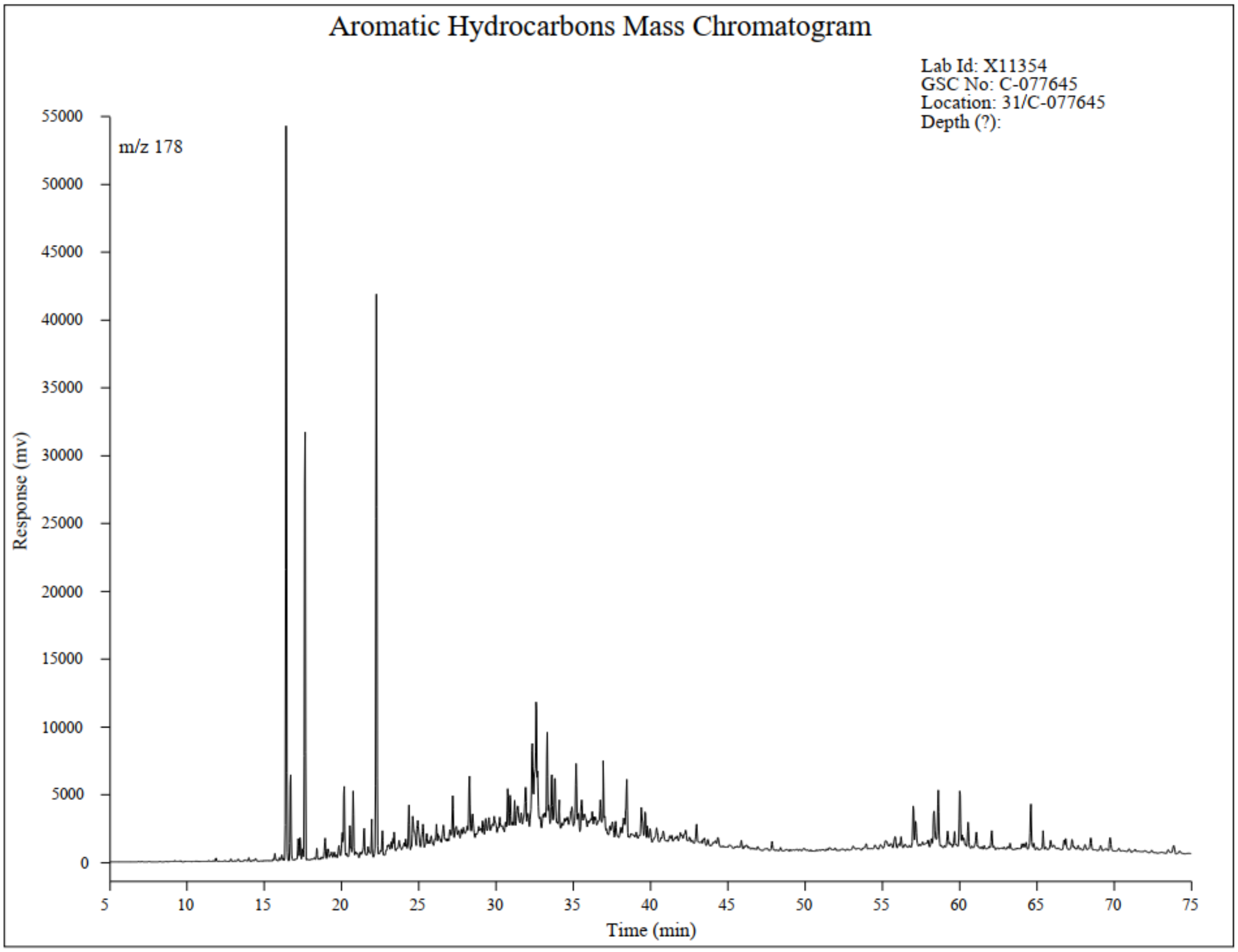

Figure B-7: Aromatic Hydrocarbons Mass Chromatogram

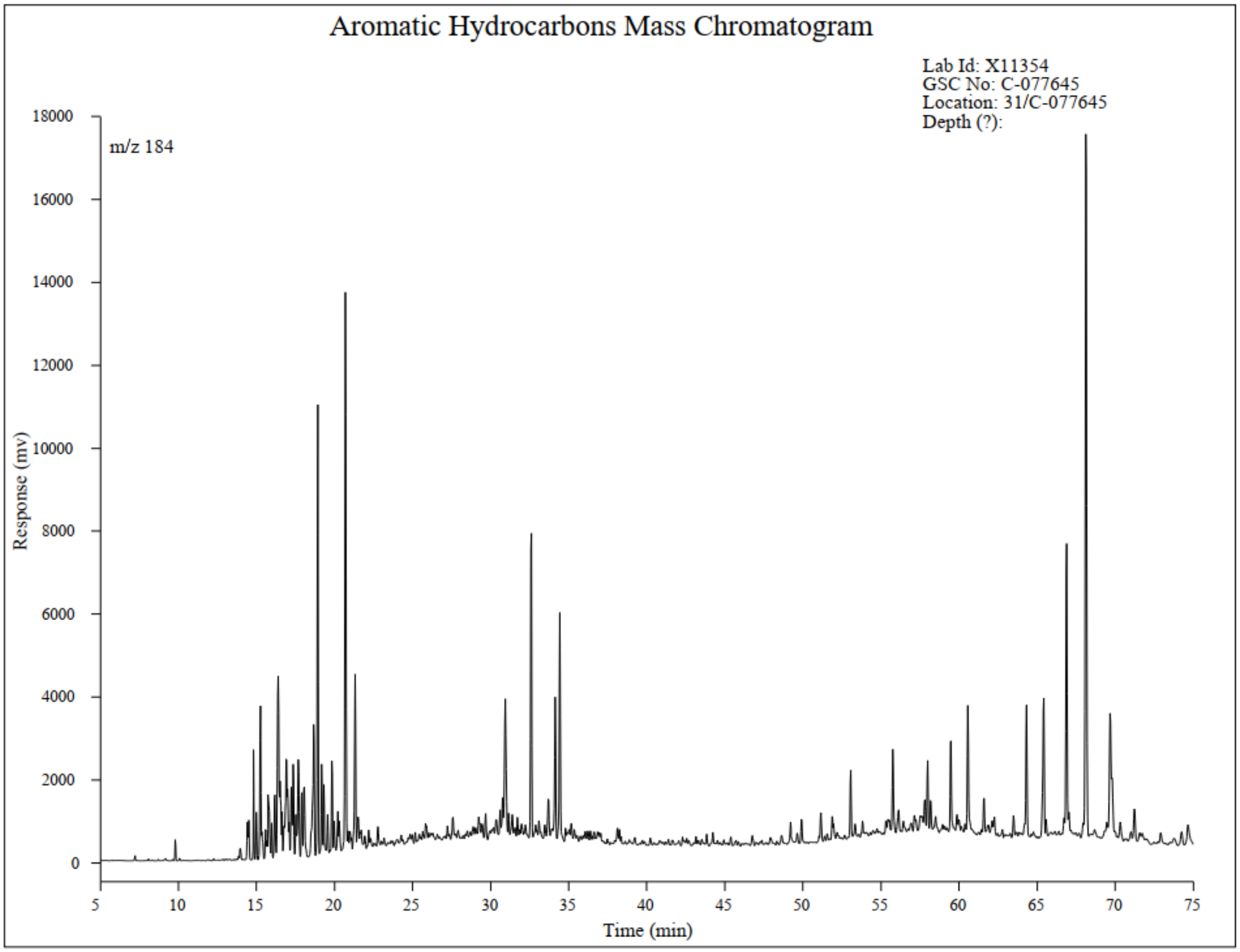

Figure B-8: Aromatic Hydrocarbons Mass Chromatogram

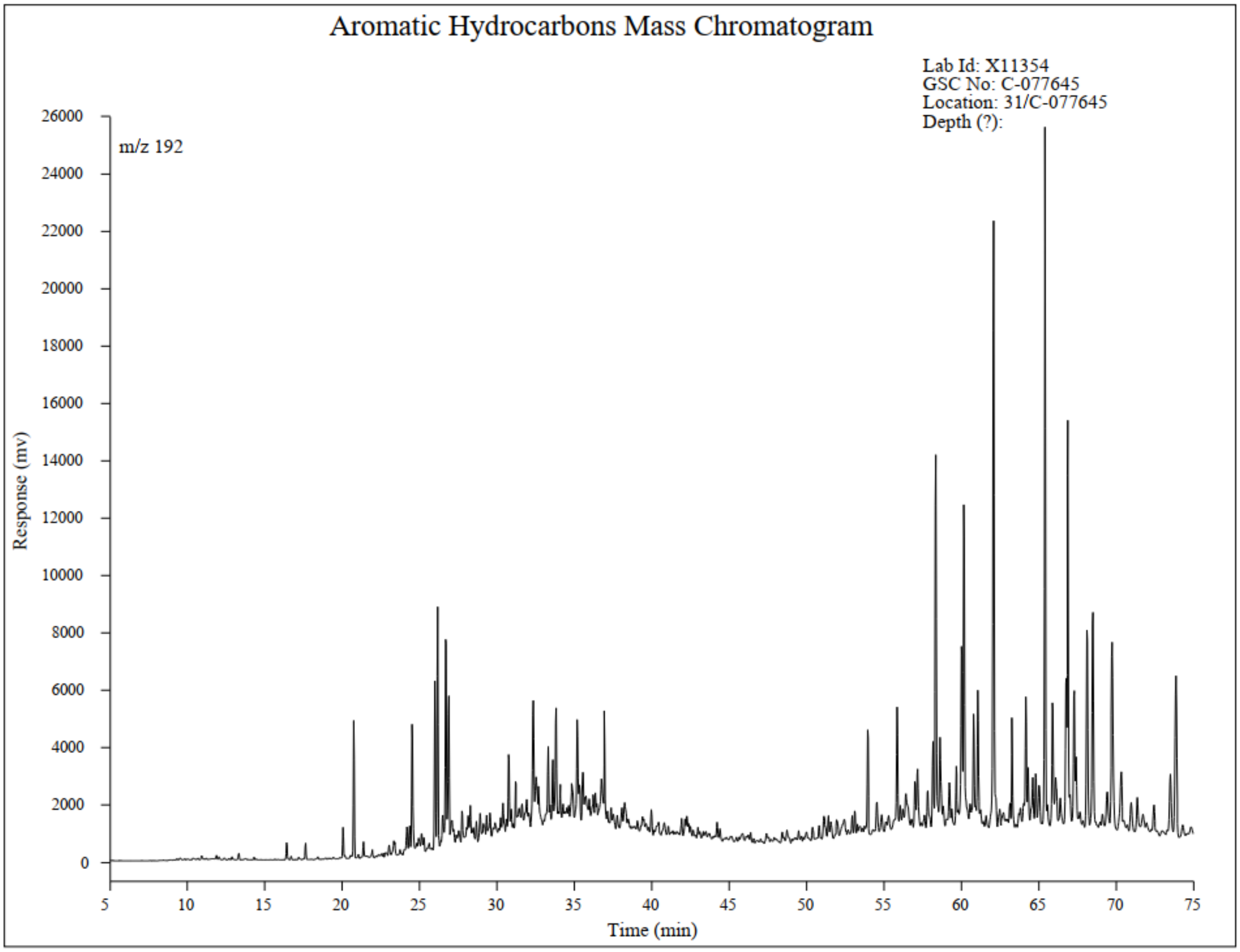

Figure B-9: Aromatic Hydrocarbons Mass Chromatogram

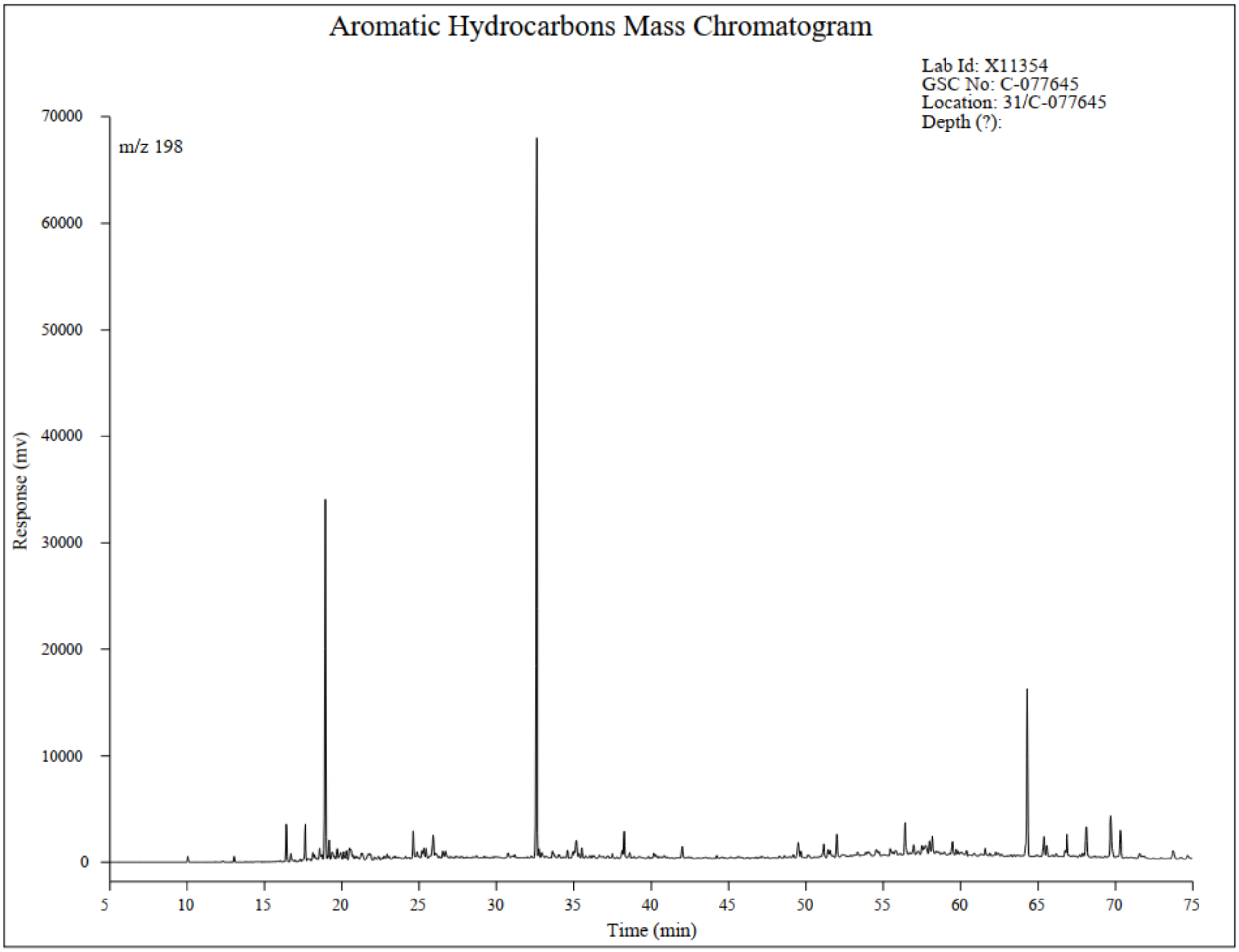

Figure B-10: Aromatic Hydrocarbons Mass Chromatogram

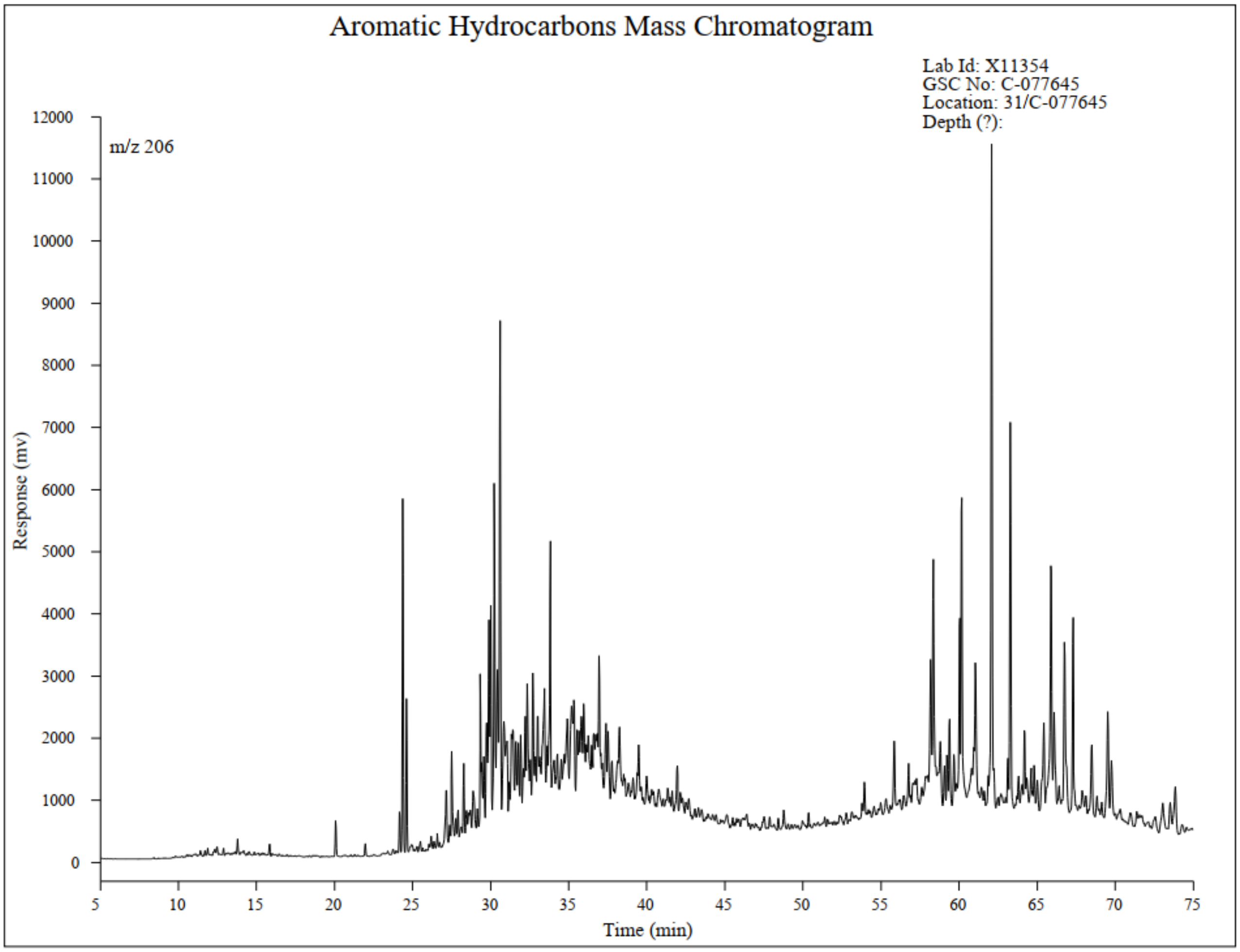

Figure B-11: Aromatic Hydrocarbons Mass Chromatogram

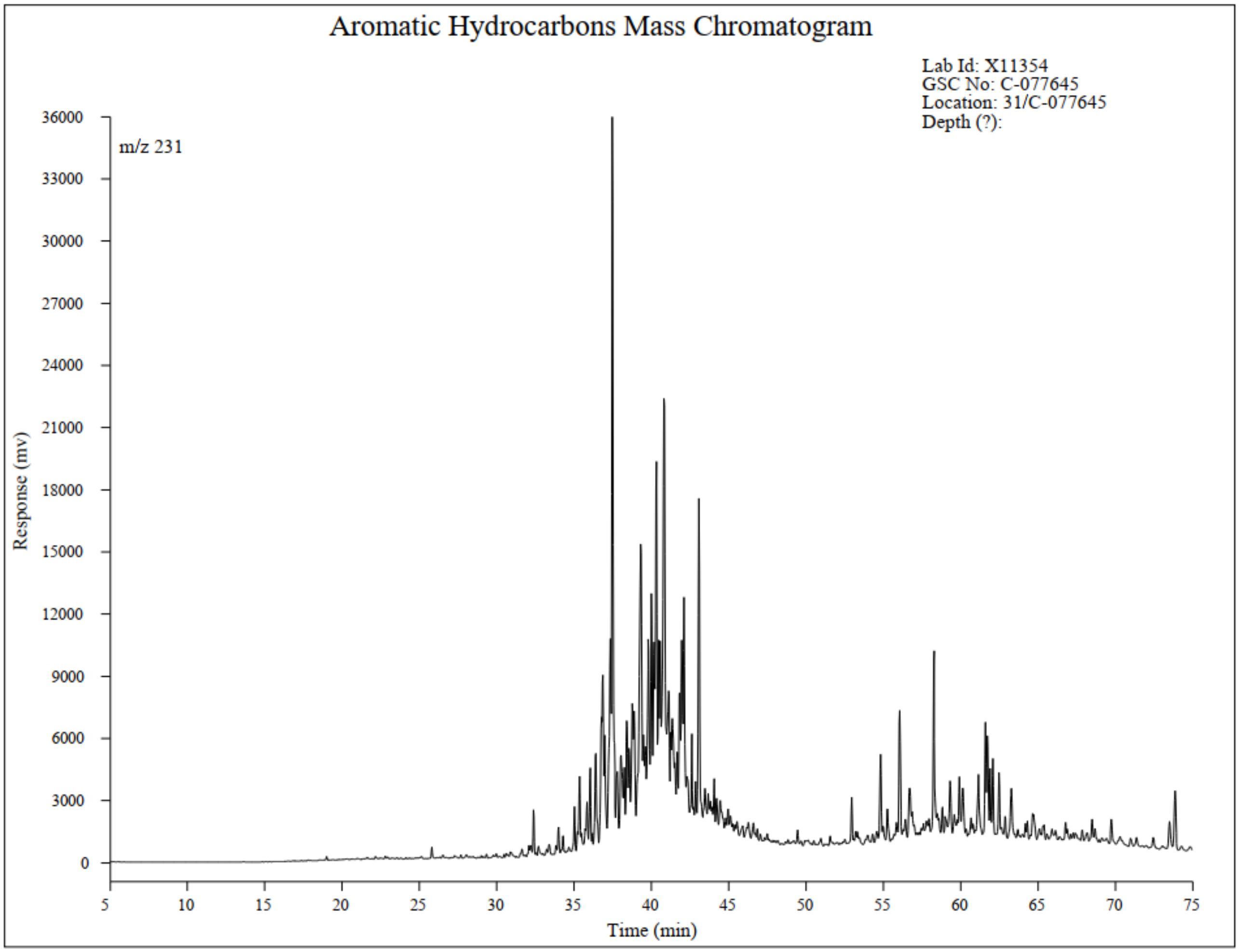

Figure B-12: Aromatic Hydrocarbons Mass Chromatogram

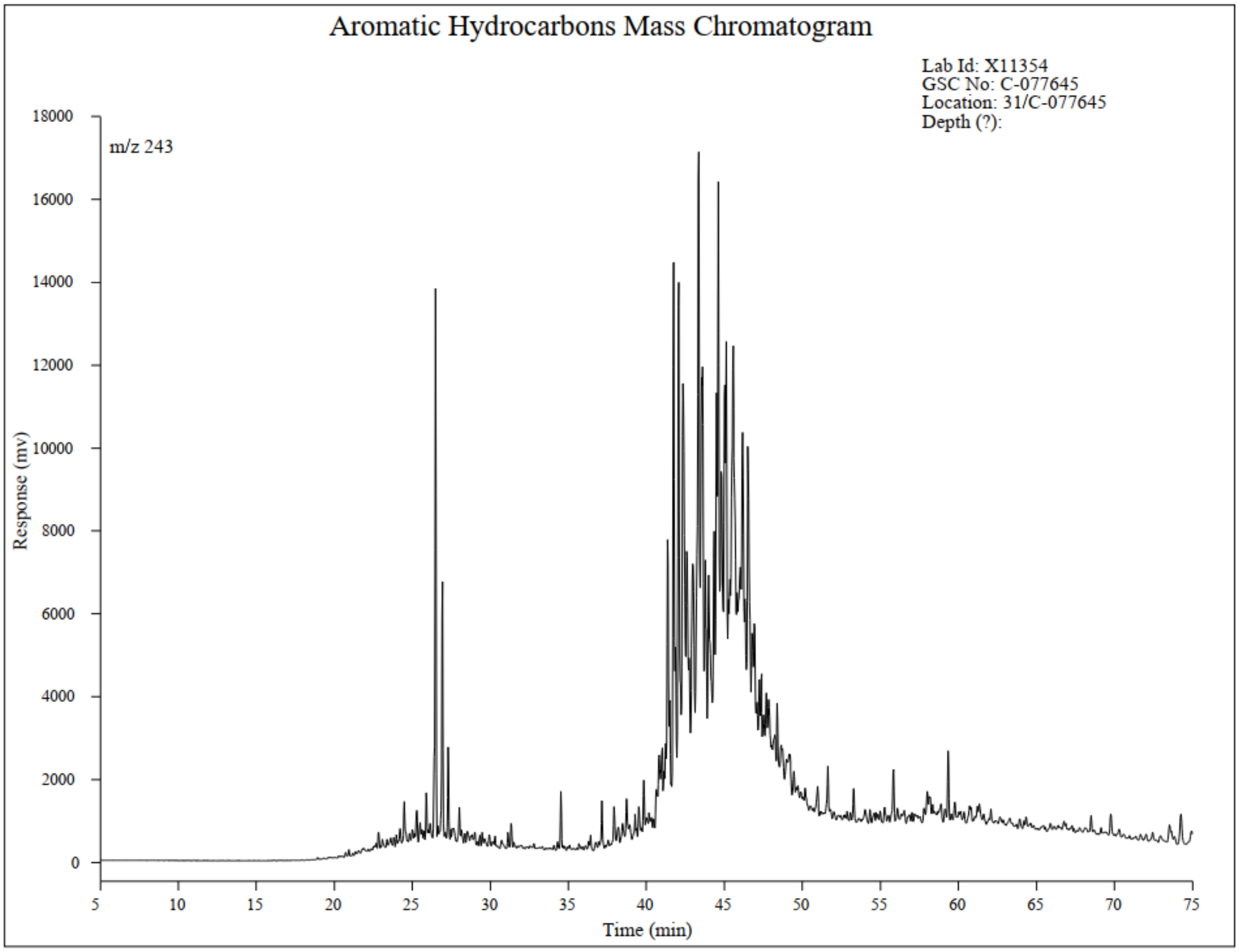

Figure B-13: Aromatic Hydrocarbons Mass Chromatogram

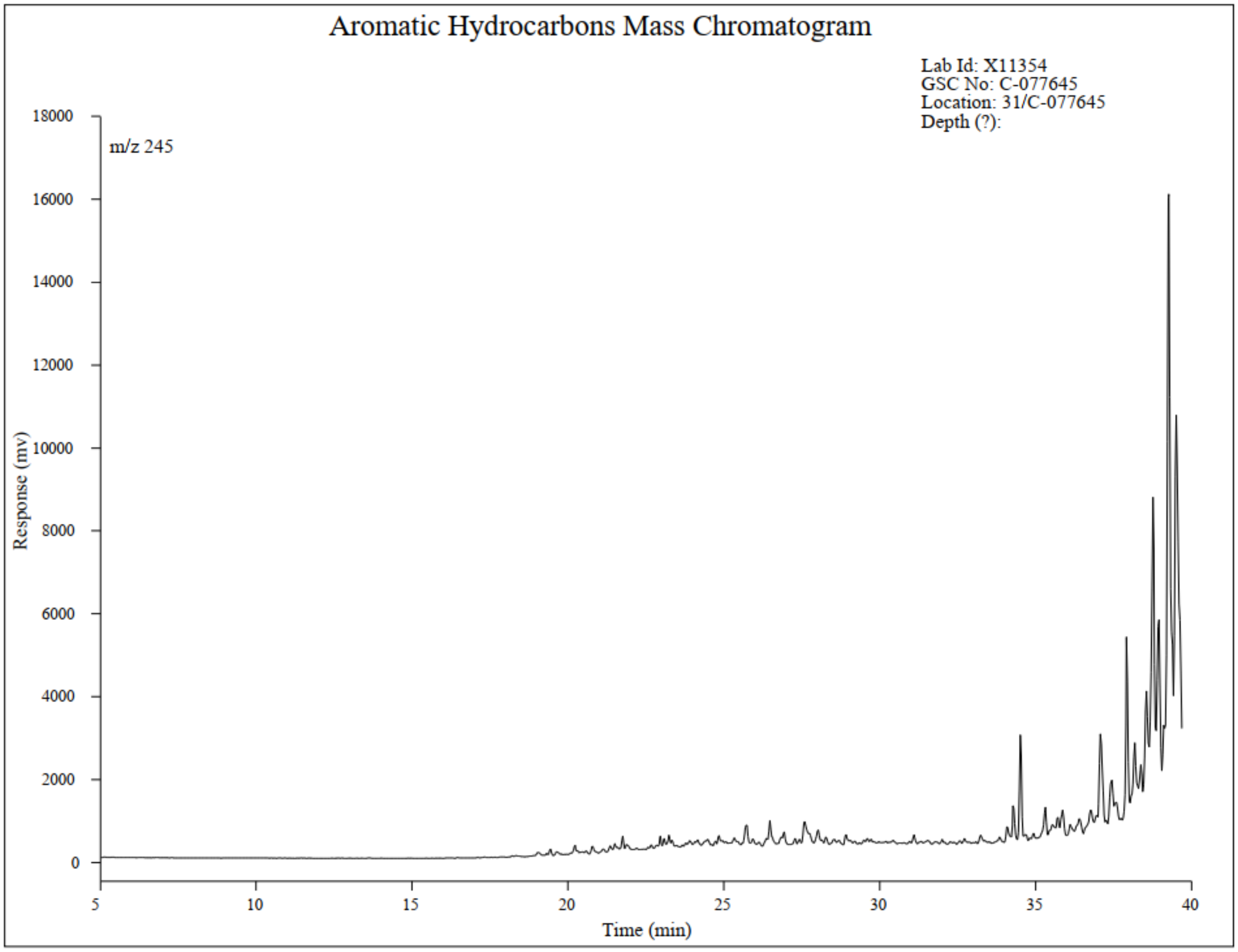

Figure B-14: Aromatic Hydrocarbons Mass Chromatogram

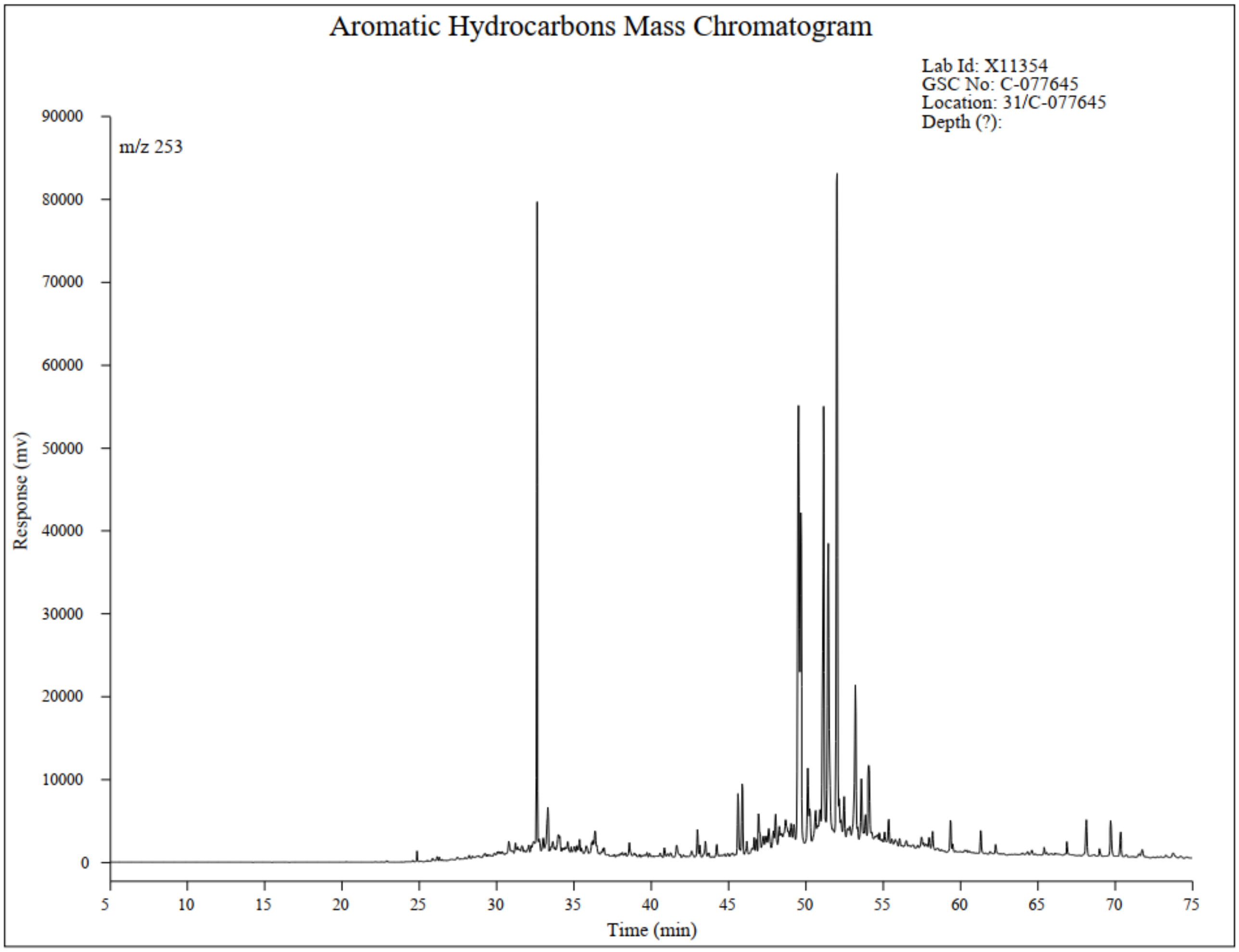

Figure B-15: Aromatic Hydrocarbons Mass Chromatogram

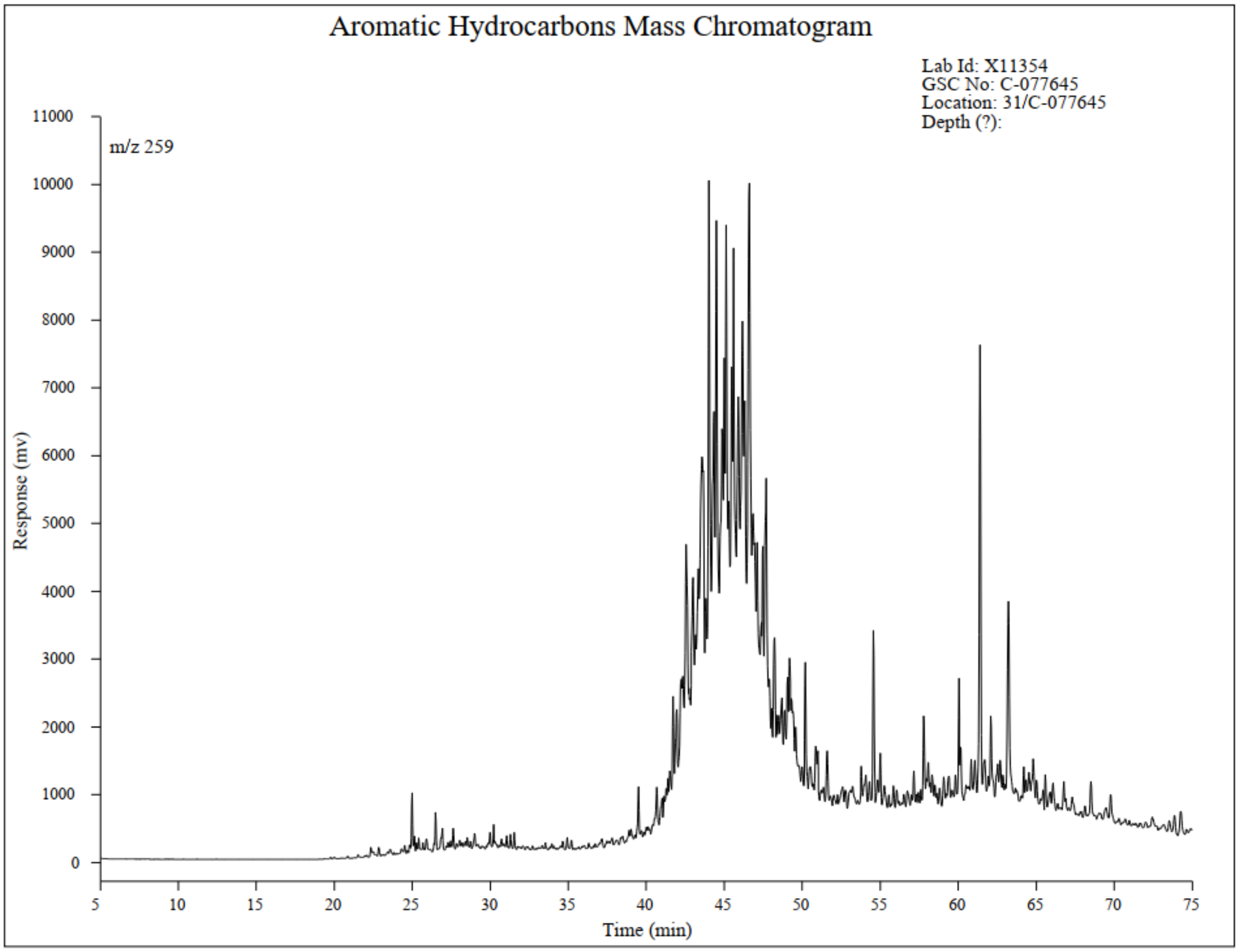

Figure B-16: Aromatic Hydrocarbons Mass Chromatogram

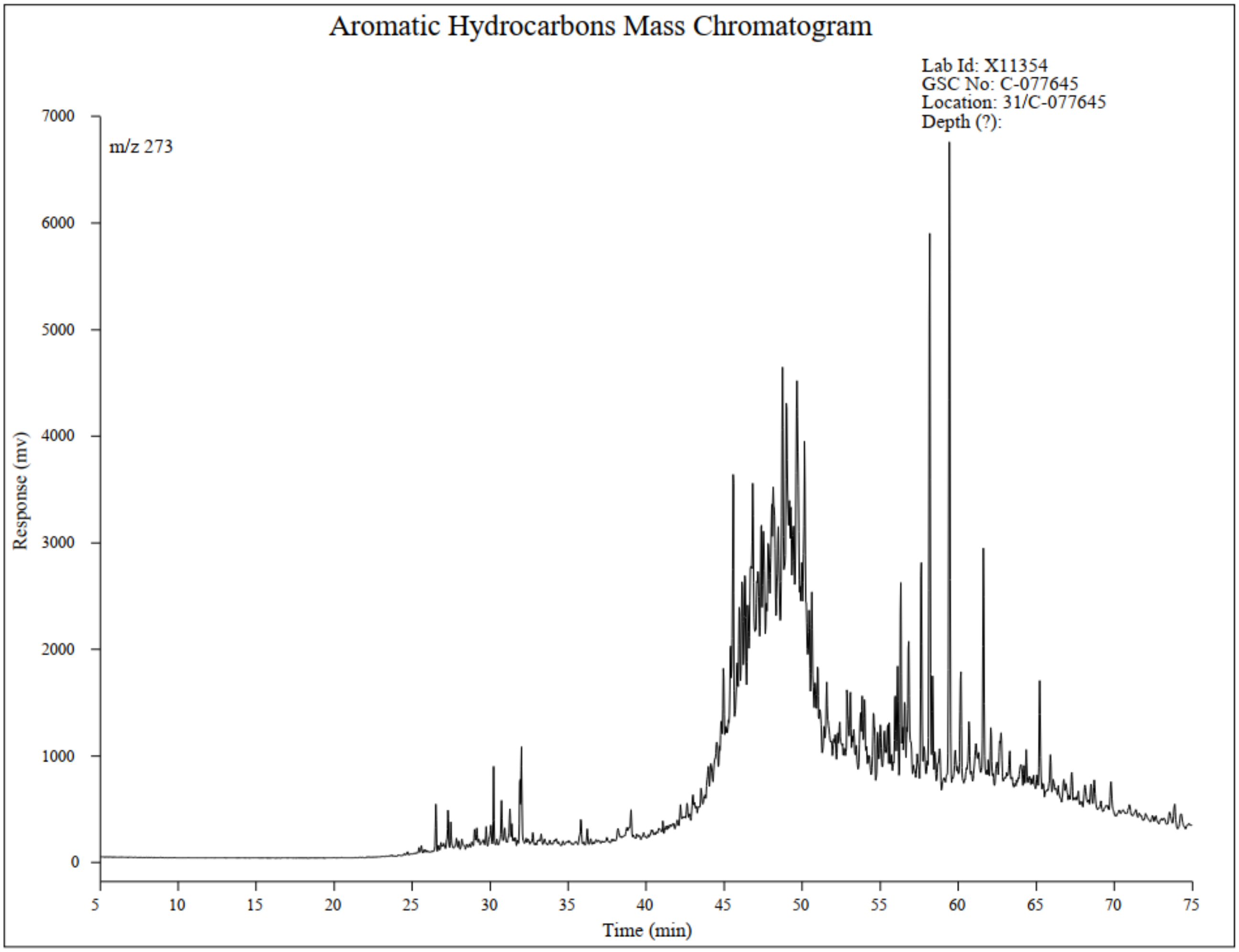

Figure B-17: Aromatic Hydrocarbons Mass Chromatogram